Ecological Indicators 128 (2021) 107810

Contents lists available at ScienceDirect

Ecological Indicators

journal homepage: www.elsevier.com/locate/ecolind

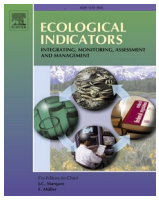

Comparative evaluation of geospatial scenario-based land change simulation models using landscape metrics

Aman Arora [a,b], Manish Pandey [b,c], Varun Narayan Mishra [d,*], Ritesh Kumar [e], Praveen Kumar Rai [f], Romulus Costache [g], Milap Punia [h], Liping Di [i]

[a] DST- Mahamana Centre of Excellence in Climate Change Research, Institute of Environment and Sustainable Development, Banaras Hindu University, Varanasi 221005, Uttar Pradesh, India
[b] University Center for Research & Development (UCRD), Chandigarh University, Mohali 140413, India
[c] Department of Civil Engineering, Chandigarh University, Mohali 140413, India
[d] Centre for Climate Change and Water Research, Suresh Gyan Vihar University, Jaipur 302017, India
[e] Haryana Space Applications Centre (HARSAC), CCS HAU Campus, Hisar 125004, India
[f] Department of Geography, K.M.C. Language University, Lucknow 226013, India
[g] Department of Civil Engineering, Transilvania University of Brasov, 5, Turnului Str, 500152 Brasov, Romania
[h] Centre for the Study of Regional Development, Jawaharlal Nehru University, New Delhi 110067, India
[i] Center for Spatial Information Science and Systems, George Mason University, 4400 University Drive, MSN 6E1 Fairfax, VA 22030, USA

ARTICLE INFO

Keywords:
Land use/ land cover
Markov chain
Land change model
Simulation
Landscape metrics

ABSTRACT

Assessing the performance of land change simulation models is a critical step when predicting the future landscape scenario. The study was conducted in the district of Varanasi, Uttar Pradesh, India because the city being "the oldest living city in the world" attracts a vast population to reside here for short and long-term, leaving the city's ecosystem more exposed to fragility and less resilient. In this work, an approach based on landscape metrics is introduced for comparing the performance of the ensemble models designed to simulate the landscape changes. A set of landscape metrics were applied in this study that offered comprehensive information on the performance of scenario-based simulation models from the viewpoint of the spatial ordering of simulated results against the related reference maps. A supervised support vector machine classification technique was applied to derive the LULC maps using Landsat satellite images of the year 1988, 2001, and 2015. The LULC maps of 1988 and 2001 were used to simulate the LULC scenario for 2015 using three Markov chain-based simulation models namely, multi-layer perceptron-Markov chain (MLP_Markov), cellular automata-Markov chain (CA_Markov), and stochastic-Markov chain (ST_Markov) respectively. The mean relative error (MRE), as a measure of the success of simulation models, was calculated for metrics. The MRE values at both the class and landscape levels were accounted for 21.63 and 11.45% respectively using MLP_Markov simulation model. The MRE values at both the class and landscape levels were accounted for 39.61 and 28.31% respectively using CA_Markov simulation model. The MRE values at both the class and landscape levels were accounted for 55.36 and 45.75% respectively using ST_Markov simulation model. The MRE values considered at class and landscape levels are further evaluated qualitatively for comparing the performance of simulation models. The results indicate that the MLP_Markov performed excellently, followed by CA_Markov and ST_Markov simulation models. This work showed an ordered and multi-level spatial evaluation of the models' performance into the decision-making process of selecting the optimum approach among them. Landscape metrics as a vital characteristic of the utilized method, employ the maximum potential of the reference and simulated layers for a performance evaluation process. It extends the insight into the main strengths and drawbacks of a specific model when simulating the spatio-temporal pattern. The quantified information of transition among landscape categories also provides land policy managers a better perception to build a sustainable city master plan.

* Corresponding author.
E-mail address: varunnarayan.mishra@mygyanvihar.com (V.N. Mishra).

https://doi.org/10.1016/j.ecolind.2021.107810
Received 27 July 2020; Received in revised form 13 May 2021; Accepted 16 May 2021
Available online 22 May 2021

1. Introduction

Land use/land cover (LULC) pattern controlled by both natural and socio-economic processes, offers an inclusive understanding of the interactions and associations of Earth's terrestrial surface with anthropogenic activities (Mmbaga et al., 2017). LULC changes (LULCC) have emerged as one of the most profoundly human-induced impacts on the Earth's ecological system. Analyzing the origins, procedures and outcomes of LULCC in addition to the relation between human-induced activities and land-use systems is acknowledged as the fundamental research topics in landscape ecology (Wu and Hobbs, 2002). In the last few decades unprecedented industrialization and persistent rapid urbanization lead to LULCC that have emerged as the primary underlying drivers impacting on ecology, agriculture, biodiversity, climate, wildlife and regional habitats from global to regional scales (Foley et al., 2005; Szilassi et al., 2006; Chapman et al., 2017; Sallustio et al., 2017; Ostad-Ali-Askari et al., 2017, 2019, 2020; Ostad-Ali-Askar et al., 2018; Li et al., 2020; Gupta and Sharma, 2020). Therefore, it is well worth investigating the spatio-temporal dynamics of LULC, which aims at providing planned decision for promoting sustainable management of natural resources.

Spatial modelling and simulation have become an effective method to analyze LULCC and have also helped in deciding how it would impact various components of the Earth's ecological system (Capitani et al., 2019). A variety of models has been extensively introduced and exploited to simulate and predict the spatio-temporal LULC dynamics worldwide and become a focal point among the researchers (Sakieh et al., 2015; Mishra and Rai, 2016, Yao et al., 2017; Guidigan et al., 2019; Gupta and Sharma, 2020). These models provide an insightful understanding of the driving forces to predict the future changes among LULC categories involving different scenarios or aspects for any region (Camacho Olmedo et al., 2018). However, modelling and simulation of LULCC comprise the complexity of not only natural constraints but also human drivers (Le et al., 2008). So, understanding the drivers of LULCC is obligatory to reduce and manage their impacts on the natural environment (Turner, 2010; Kolb et al., 2013). The spatio-temporal change analysis is a complex and nonlinear practice with the specific direct and indirect drivers at various scales that are very diverse (Lambin et al., 2003; Kolb et al., 2013). The competency of a model and its success rate depends on the studying or involvement of driving factors, cross-scale dynamics, various levels and sub-levels of analysis, spatial relations and neighbourhood effects, integration level, and temporal changing direction of landscapes and its drivers (Lambin et al., 2003; Verburg et al., 2004; Bürgiet al., 2004; Eastman et al., 2005; Kolb et al., 2013). The complexity, inherent dynamic characteristics, and ambiguity of natural systems require a conceptualized demonstration of sustainable LULC practices based on modelling processes in rapidly growing regions.

Satellite-based remote sensing (RS) technologies and Geographical Information System (GIS) with the enormous development brought more opportunities in spatial landscape planning and management practices. Using remotely sensed data is as an effectual way to generate a diverse set of temporal LULC maps at different observational scales (Mishra and Rai, 2016; Yao et al., 2017; Mishra et al., 2018; Du et al., 2018; Tang and Di, 2019). Thus, it is very beneficial to improve the understanding and modelling of LULC change processes. The significant development has been witnessed in the field of LULCC simulation and modelling with ever-increasing availability of data from remote sensing and other sources. The operations of improved statistics, coupled with advanced mathematical algorithms, have enhanced the performance and prediction rate of LULCC simulation models. A variety of spatially-explicit land change models have been widely introduced and exploited to simulate future landscape scenarios in different regions around the world (Mitsova et al., 2011; Arsanjani et al., 2013; Sakieh and Salmanmahiny, 2016; Mishra and Rai, 2016; Yao et al., 2017; Mishra et al., 2018; Islam et al., 2018; Kantakumar et al., 2019; Varga et al., 2019; Cao et al., 2020). The land change simulation models compatible with remotely sensed data have been used as well to mimic the dynamic processes of LULCC under different scenarios (Hamad et al., 2018; Liu et al., 2019). These models are considered as reliable tools for analyzing the dynamic process of LULC conversion with reasonable accuracy and providing insights concerning management alternatives. Each land change simulation model has its drawbacks and strengths reported by Triantakonstantis and Mountrakis (2012). So, it is required to overcome the inadequacies of each model by coupling them to work as complementary to each other. In several studies, the performance of coupled modelling methods has been evaluated for LULCC simulation and future landscape prediction (Arsanjani et al., 2013; Bozkaya et al., 2015; Dezhkam et al., 2017; Mishra et al., 2018; Nasiri et al., 2019; Varga et al., 2019).

Performance appraisal of land change models is an essential step while simulating the dynamic phenomenon of LULC transformation. Several methods including simple least squares regression (Rafiee et al., 2009), kappa-based statistics (Pontius and Millones, 2011; Mishra and Rai, 2016), and receiver operating characteristic (ROC) curve (Pontius and Batchu, 2003; Pontius and Si, 2014) are available for evaluating the performance of land change simulation model. In some studies, the accuracy of the simulation process is performed by comparing the output map at the ending time of the validation interval to the reference map at the same time (Mishra and Rai, 2016; Chakraborti et al., 2018). The individual method has its merits and demerits used to provide numeric signatures about the information on the agreement between the predicted outputs and the actual reference input layer (Sakieh and Salmanmahiny, 2016). The kappa-based measures are not suitable for quantity-based accuracies, having a probability of producing misleading information as described by Pontius and Millones (2011). It is observed that the two-map comparison in case of persistence landscape, typically gives large values for percent correct and kappa, irrespective of correctly simulated changes (Varga et al., 2019). The simple least squares regression methods and ROC curve is not assumed to provide spatial information of LULC patterns in terms of an agreement between two thematic maps. One of the significant drawbacks of these methods is their inability to provide details of the morphological contract found between simulated and reference maps (Dezhkam et al., 2017). Therefore, Performance appraisal of simulation models based on spatially-explicit method has achieved great attention and priority. Spatial metrics powerful tools in assessing simulation success, are the quantitative measure of landscape characteristics at both composition and configuration levels. Spatial landscape metrics based on landscape ecology, are valuable tools in mapping and quantifying LULC characteristics. The landscape metrics are commonly used in ecological investigations (Peng et al., 2010; Frazier and Kedron, 2017). However, they are now being extended to enhance the understanding of LULC change processes at the landscape level. Several studies have exhibited the utilization of the landscape metrics in describing spatio-temporal LULC dynamics (Paudel and Yuan, 2012; Asgarian et al., 2014; Smiraglia et al., 2015; Kumar et al., 2018). However, minimal information is available regarding the validation and evaluation of the land change simulation models using landscape metrics. Wu et al. (2009) assessed the SLEUTH model by applying multi-method and reported that the method based on landscape metrics was profoundly best for analysis and assessment of the modelling outputs. Sakieh and Salmanmahiny (2016) assessed the performance of a scenario-based GEOMOD model to validate the simulative outputs. In some studies, the performance of an integrated CA_Markov simulation model was evaluated with the help of landscape metrics indicating close agreement between simulated and reference layers (Guan et al., 2011, Amiri et al., 2017, Dezhkam et al., 2017). However, the number of studies comparing the performance of multiple integrated models for land change simulation-based on landscape metrics is limited. The studies discussed in the above paragraphs reveal that there are only a limited research works which focused on the ensemble of more than one land change simulation models to assess the enhancement in their performance. And there are rarer studies which

compared the performance of two or more ensemble models for their ability to simulate the LULC changes over the spatial and temporal scales. Thus, this study attempts to fill this gap by incorporating three ensemble models viz. MLP_Markov, CA_Markov, and ST_Markov for the purpose of comparing their performances in LULC simulation in the Varanasi district of Uttar Pradesh, India. Furthermore, since Varanasi is the "oldest living city in the world" (Prajapati and Tripathi, 2008; Shukla, 2013; Reynolds, 2014; Omar et al., 2020), experiences huge population influx, for both short term and long term, and hence faces danger of disturbance in the fragile floral and faunal ecosystems. Therefore, analyzing the transitions among LULC categories using advanced ensemble models and comparing their performances is another novel issue that this study undertakes.

For the above stated reason, the present work selected the main urban area of Varanasi district, India as the study site. This area has experienced a high growth rate in the population and fast urbanization in the last few decades. This study offers a sequence of analyses to overcome the frequent problems associated with the identification of spatial drivers of specific LULC change processes and examines how these drivers can be translated into accurate land change simulation. More specifically the present study aims to (1) use and analyze different landscape metrics during the land change simulation process based on the geospatial scenario; (2) compare the performance of three integrated simulation models, i.e., ST_Markov, CA_Markov, and MLP_Markov based on landscape metrics. The outcomes of this work could provide valuable insights into the spatial pattern of LULCC and the validation of simulated maps. These geospatial scenario-based models applied to simulate changes occurred in landscape structure are of great attention to policymakers, land managers and local authorities to use land resources sustainably.

2. Study site

Varanasi district (Uttar Pradesh), India (Fig. 1), Geographically lying between 25° 10′ to 25° 37′ N latitude and 82° 39′ to 83° 10′ E longitude, and covering an area of 1532.91 km^2 has been chosen to be the study site for this work. It is situated on the bank of holy river Ganga. This part of the Ganga River Basin, being agriculturally very productive region, is sculpted due to interplay of climate, tectonics, and anthropogenic factors (Pandey, 2014; Arora et al., 2018, 2019) and replenished with annual soil-forming ingredients by several major rivers and their tributaries (Raju et al., 2015; Raju and Pandey, 2013). It experiences humid subtropical climatic condition with considerable variation between summer and winter temperature and rainfall. It is also well-known for religious conviction and cultural activities for many decades. The Ganga river and its tributaries like Gomati, Varuna along with many numbers of natural and artificial ponds represent the waterbody component in the present study area (Mishra et al., 2018). Raju and Bhatt (2015) pointed out that 118 ponds have been reported to be existing in the Varanasi city itself. Because of annual flooding in the rivers, soil along the active floodplain is recharged with younger alluvium and older alluvium is found in the upland areas (Singh and Singh, 1971). Singh (2015) in his extensive study of flora of Varanasi district reported 1015 plant species of 601 genera related to 116 families. Varanasi is densely populated area in the because of its location on the bank of the most fertile Ganga river, existence of various educational institution, being the oldest surviving religious city of the world, etc. and these factors lead to dynamic nature of the land use/ land cover transitions.

3. Materials and methodology

The satellite images from different sensors, e.g., Landsat-TM, Landsat-ETM+, and Landsat-OLI acquired on 4 November 1988, 31 October 2001, and 15 November 2015 respectively, were used for land change simulation purpose. All the satellite images were downloaded from the official website of USGS earth explorer (http://earthexplorer.usgs.gov/), respective details of which are given in Table 1. The slope and aspect were computed using SRTM DEM with 90 m version 3. The toposheet and Google Earth images were used to extract road and

Table 1
List of satellite data applied in this study.

Satellite-sensor	Path/row	Acquisition date	Product type
Landsat 5-TM	142/42, 142/43	4 November 1988	L1T
Landsat 7-ETM+	142/42, 142/43	31 October 2001	L1T
Landsat 8-OLI/TIRS	142/42, 142/43	15 November 2015	L1T

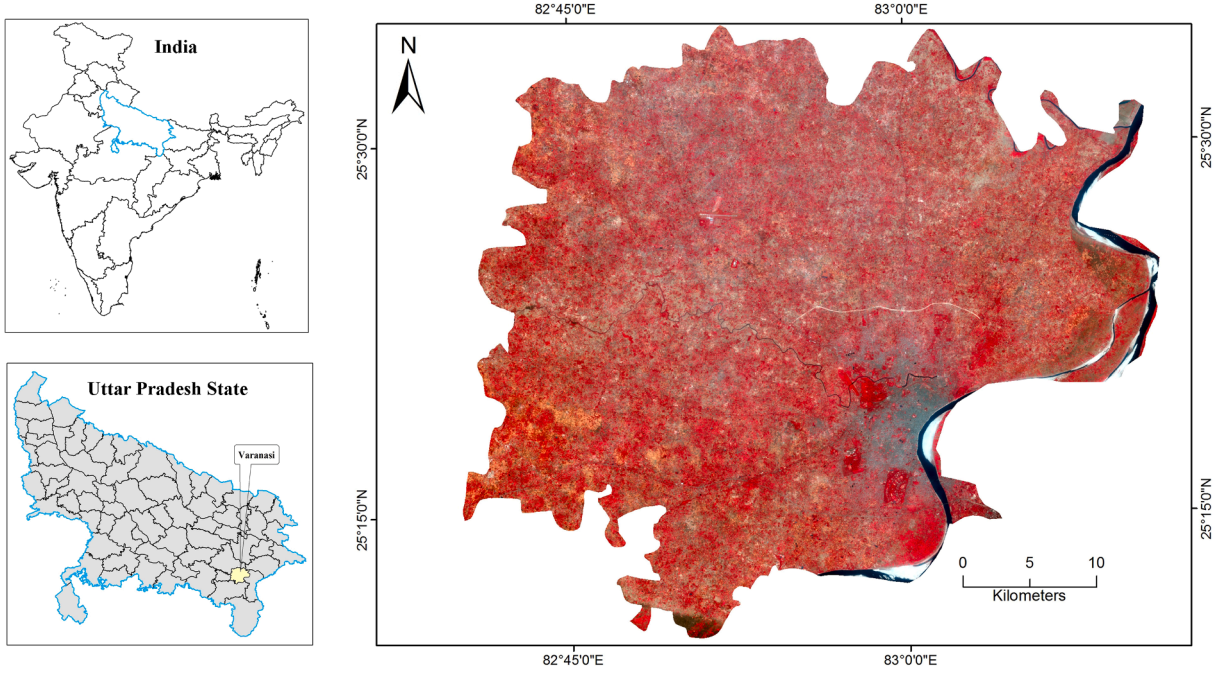

Fig. 1. Location Map of the study site as viewed on Landsat 8-OLI data.

railway layers.

The ENVI (v. 5.1) software was used for pre-processing, interpretation and LULC classification of satellite images. The landscape metrics were calculated by utilizing FRAGSTATS (v.4.2.1) software. In this work, the integrated land change simulation models such as ST_Markov, CA_Markov, and MLP_Markov were applied using the IDRISI Selva software. The CROSSTAB module available in the IDRISI software was used to generate a cross-tabulation table between two images for observing the reliability of images and distribution of pixels between the LULC categories. The Markov chain (MC) analysis is one of the most commonly used stochastic methods in simulation and modelling processes. In this study, the estimated quantities in 2015 are based on the transitions during 1988–2001, using the MARKOV module of IDRISI. The land change simulation was performed using the CA_MARKOV module and MLP_Markov architecture available in the Land Change modeler (LCM) component of IDRISI. The transition probability matrix provided by MC is used during the simulation CA_Markov and MLP_Markov simulation models.

3.1. Pre-processing and LULC classification of satellite images

First of all, the multi-temporal Landsat images were imported into ENVI platform and layer-stacked all the spectral bands. The QUick Atmospheric Correction (QUAC) method available in the ENVI software, was applied to perform atmospheric correction of multi-temporal Landsat satellite images. The image-to-image registration method was utilized to co-register all the datasets to the Universal Transverse Mercator projection system (UTM), Zone 44 North, WGS 1984 datum. The first-degree polynomial equation and nearest-neighbor resampling technique was used to set the pixel size at 30 m. After that, spatial subsetting was performed to extract the area under investigation. The false-colour composites (FCCs) of all the images were produced using the appropriate band combination. These FCCs were utilized for the analysis and creation of training sites for individual LULC category. The transformed divergence (TD) method-based separability analysis was applied to examine the quality of training sites before the LULC classification. The training and testing datasets comprising various LULC categories were collected from diverse locations in the study area using a random sampling method.

The LULC maps of the years 1988, 2001 and 2015 were produced by applying support vector machine (SVM) classification method. Seven broad LULC categories for instance, agriculture, fallow land, sparse vegetation, dense vegetation, urban, sand, and water bodies, were prepared according to the landscape of the study site. The accuracies of produced LULC maps were evaluated by applying measures such as producer's accuracy (PA), user's accuracy (UA), and overall accuracy as prescribed by Congalton and Green (1999). The change analysis for all the LULC products during the periods defined as 1988–2001, 2001–2015, and 1988–2015 was also performed.

3.2. Analysis of landscape metrics

In order to measure the changing LULC patterns within the study region, landscape indices were computed with the help of FRAGSTATS 4.2.1 software (McGarigal et al., 2002). In the last few decades, there has been an increasing number of statistical measures used for attributing landscape composition (Cushman et al., 2008). Several metrics have been evolved for describing the spatial pattern of landscapes at composition and configuration levels (Kong et al., 2012; Smiraglia et al., 2015; Kumar et al., 2018). But the metric selection is hampered by inherent redundancy and similar information of the metrics themselves. Some most frequently used class level and landscape-level metrics (Jaafari et al., 2015; Sakieh and Salmanmahiny, 2016; Dezhkam et al., 2017) were calculated for all the classified images. For each of the seven major LULC classes, seven metrics depicting different features of the landscape mosaic, including the total class area (CA), number of patches (NP), mean patch area (Area_MN), edge density (ED), mean Euclidean nearest neighbour distance (ENN_MN), Landscape shape index (LSI), and largest patch index (LPI) were calculated and listed in Table 2. The structure of a landscape affects its function and practices (Farina, 2006). A more comprehensive description of the metrics used in this work is given by McGarigal et al. (2012).

3.3. Land change simulation modelling

In the present study, historical growth scenario was used to perform model calibration and simulation of LULCC for the study area under investigation. The simulation of structural changes and transitions in landscapes are gaining a lot of interests by remote sensing community. This study employed three scenario-based hybrid simulation models, namely ST_Markov, CA_Markov, and MLP_Markov, to evaluate their performance and success in view of measuring the spatial agreement between the patterns of reference and simulated data. The working flow chart adopted in the study is illustrated in Fig. 2.

The Markov chain (MC) analysis is one of the most commonly used tools for describing the behavior of complex systems. The theoretical basis of MC analysis is originated through the practice of creating Markov random systems for optimized control and anticipation (Aaviksoo, 1995; Jiang et al., 2009; Pirnazar et al., 2018). The MC model quantifies the conversion and transfer rate between various LULC types (Mirkatouli et al., 2015; Tsarouchi et al., 2014). It computes the changing probability of a pixel from a landscape type to a different using the observed data within a particular time period. It leads to the formation of a transition probability matrix which is assumed to be spatially independent (Brown et al., 2000; Eastman, 2006). However, the propensity of a changing pixel is not only based on its present status but also affected by its neighboring pixels. As a result, a stand-alone MC model does not describe a spatially distributed changing pattern of LULC types (Araya and Cabral, 2010). Therefore, it needs to integrate MC with other models for overcoming the inadequacy to work as complementary to each other.

The first simulation model is ST_Markov that integrates both stochastic and Markov chain algorithms. The MC analysis was performed before stochastic processes between LULC layers of the year 1988 and 2001 to simulate and predict the LULC scenario for the year 2015. The LULC maps of two dates (1988–2001) were analyzed to generate a transition probability matrix (Table 3), a transition area matrix (Table 4), and Markov conditional probability images (Fig. 3). After that, all the Markov conditional probability images were combined into a single image for simulating and predicting future scenario (Mishra et al., 2018).

The second simulation model is CA_Markov that integrates both cellular automata and Markov chain algorithms. The MC model does not consider spatial contiguity in different types of LULC transformations that are likely to occur (Eastman, 2006). Therefore, the CA-MC model was used to integrate the probable spatial information of transitions to the MC process. For running the CA_Markov, initial LULC map of the year 1988, the transition area matrix, the transition probability matrix, and transition probability images were applied. The CA_Markov simulation model is not able to reveal the constraints and driving factors of LULCC (Eastman, 2006). So, a 5×5 CA contiguity filter was applied for assigning low suitability scores to the inaccessible cells (Mitsova et al., 2011; Salehi-Hafshejani et al., 2019). The multi-criteria evaluation method was applied to create a suitability map of individual LULC types (Fig. 4). Finally, the CA_Markov model available in IDRISI Selva software was executed to simulate the LULC for year 2015 by exploiting the Markov transition area matrix, suitability maps, the 5×5 CA contiguity filter, and the LULC map of year 2001 as base (Mishra et al., 2018).

The third simulation model is MLP_Markov that integrates both the MLP neural network and Markov chain algorithms. In this study, LCM module available in IDRISI was used to run MLP. The architecture of MLP is based on feed-forward neural network process. In general, neural

Table 2
Description of landscape metrics.

Concept	Type of metrics	Landscape metrics	Abbreviation	Range	Units
Fragmentation	Landscape composition	Number of patches	NP	NP > 0, without limit	None
Fragmentation Area	Landscape configuration	Mean patch area	AREA_MN	AREA_MN > 0, without limit	Hectare
Area	Landscape composition	Total class area	CA	CA > 0, without limit	Hectare
Density	Landscape configuration	Edge density	ED	ED ≥ 0, without limit	Meters per hectare
Isolation	Landscape configuration	Mean Euclidean nearest neighbour distance	ENN_MN	ENN > 0, without limit	Meters
Dominance	Landscape composition	Largest patch index	LPI	0 < LPI ≤ 100	Percent
Shape, aggregation index	Landscape configuration	Landscape shape index	LSI	LSI ≥ 1, without limit	None

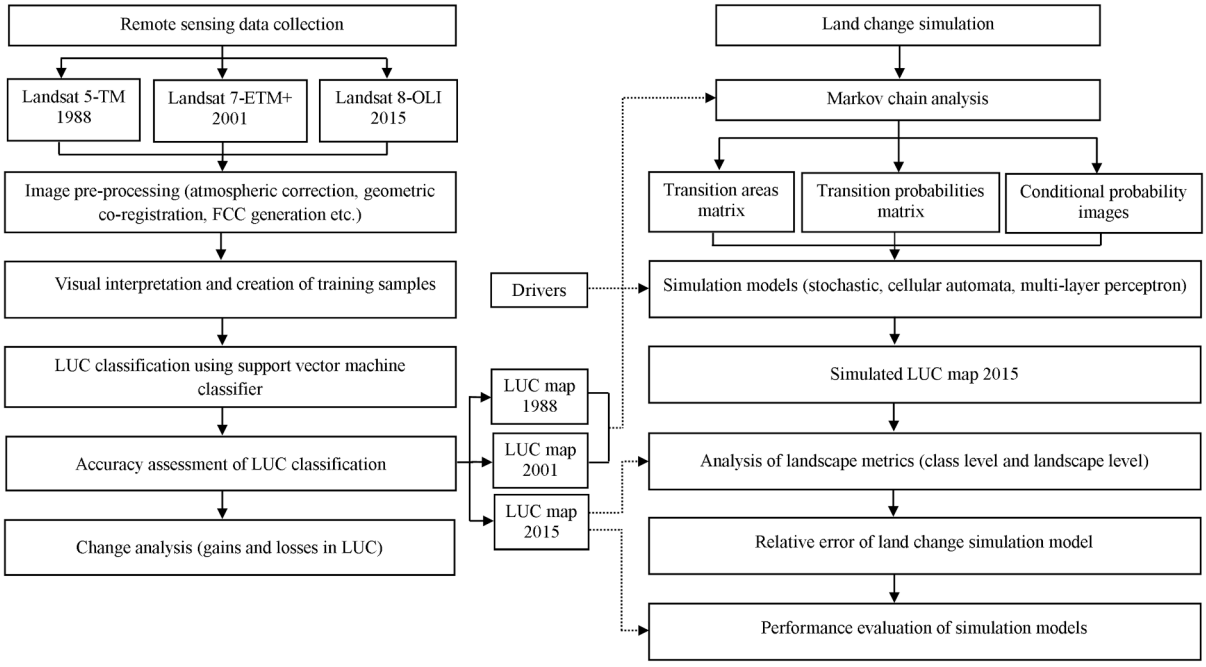

Fig. 2. Methodology Flow Chart.

Table 3
Markov transition probability matrix of LULCC during 1988–2001.

LULC category	Agriculture	Dense Vegetation	Sparse vegetation	Fallow land	Urban	Water bodies	Sand
Agriculture	0.172	0.081	0.330	0.147	0.263	0.006	0.000
Dense vegetation	0.319	0.140	0.458	0.042	0.032	0.009	0.000
Sparse vegetation	0.440	0.111	0.315	0.099	0.028	0.007	0.000
Fallow land	0.423	0.085	0.341	0.122	0.009	0.015	0.006
Urban	0.037	0.030	0.039	0.037	0.830	0.019	0.009
Water bodies	0.079	0.052	0.169	0.086	0.021	0.467	0.126
Sand	0.059	0.001	0.062	0.223	0.001	0.260	0.395

Table 4
A transition area matrix during period of 1988–2001.

LULC category	Agriculture	Dense Vegetation	Sparse vegetation	Fallow land	Urban	Water bodies	Sand
Agriculture	1,060,174	260,787	1,091,732	372,931	37,290	20,767	810
Dense vegetation	172,386	75,721	247,299	22,441	17,138	4817	0
Sparse vegetation	978,102	247,028	700,018	221,868	61,844	15,746	172
Fallow land	347,646	69,466	280,430	100,088	6918	12,198	5040
Urban	17,446	4947	34,768	7053	98,705	3079	1260
Water bodies	12,635	8380	27,295	13,804	3394	75,175	20,322
Sand	2694	46	2821	10,190	46	11,824	17,994

networks are analogous to biological neurons. It consists of multiple layers of simple computing nodes that can operate complex nonlinear systems. The MLP creates a network of neurons between the driving forces and the classes of change and persistence (Mishra et al., 2014; Mazumdar et al., 2016). The MLP neural network is capable of combining all the variables at a time, concerning the LULC transitions (Mishra and Rai, 2016). Only the main transitions among the LULC, responsible for the landscape dynamics were added in the sub-model to

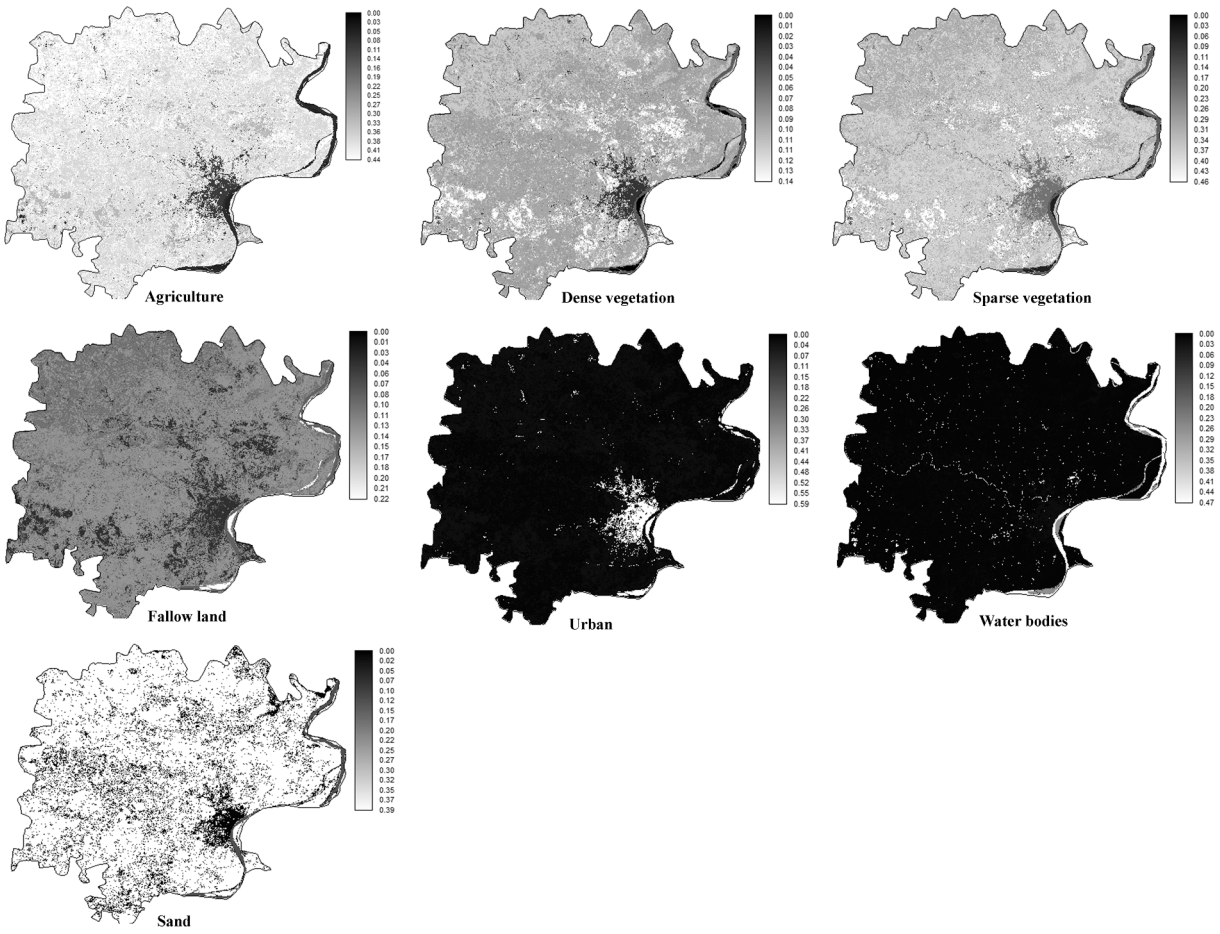

Fig. 3. Markovian images.

improve the performance of the MLP neural network (Mishra and Rai, 2016). Here, a total six environmental variables including static (elevation, slope, and aspect) and dynamic (distance from urban, distance from roads, and distance from the rail network) were considered. An empirical likelihood image as a qualitative variable was used. These seven variables (Fig. 5) were used as inputs to produce transition potential maps during MLP_Markov based simulation process. The network of major roads and railway lines were considered as constraints. The MLP neural network automatically generates a random sample of pixels during the LULC transition during the required time. In total, 50% of the samples were randomly selected as the training data, whereas remaining 50% were used as the testing data. Accuracy of 0.877, a quantification of the calibration was achieved after completing the MLP process. Finally, the simulation of the LULC scenario was executed using transition potential maps (Mishra et al., 2018).

3.4. Evaluation of model performance based on landscape metrics

Generally, the performance of a model is evaluated by comparing the reference and simulated maps. Firstly, the LULC layer for the year 2015 was generated by using ST_Markov, CA_Markov, and MLP_Markov simulation models based on transitions among classes from 1988 to 2001. The simulated outcomes were then compared with the reference LULC map derived from satellite imagery of the year 2015. The landscape metrics (Table 2) were calculated to quantify the agreement between the spatial layers of simulated and reference data. The Relative Error (RE) and Mean Relative Error (MRE) indices given by Dezhkam et al. (2017) were used for comparing the metrics derived from simulated and reference layers in order to assess the performance of simulation models. The RE and MRE values can be calculated using equations (1) and (2) as given below:

$$RE = \left[\frac{(M_p - M_r)}{M_r}\right] * 100 \quad (1)$$

where M_p and M_r are the landscape metric values derived from the simulated and reference LULC maps, respectively.

$$MRE = \frac{1}{n}\sum_{i=1}^{n} RE_i \quad (2)$$

where, RE_i = estimated relative error of simulation model for individual LULC type for each metric; n = number of all estimated relative errors.

Dezhkam et al. (2017) proposed a categorization scheme based on RE and MRE values to evaluate the success of simulation process in terms of the variation of the metrics derived from simulated and reference layers (Table 5). The RE values were further categorized into qualitative details to provide a simple and quick analysis of model performance. The LULC map strongly affects the accuracy of landscape metrics derived from it. In general classification accuracy of 85% is acceptable for LULC maps (Congalton and Green, 2009).

4. Results

4.1. LULC maps and accuracy assessment

The LULC maps based on SVM classifier, of the years 1988, 2001, and 2015 are represented in Fig. 6. The overall mapping accuracies for the LULC maps of years 1988, 2001, and 2015 were found to be 86.94, 88.84, and 89.25%, respectively.

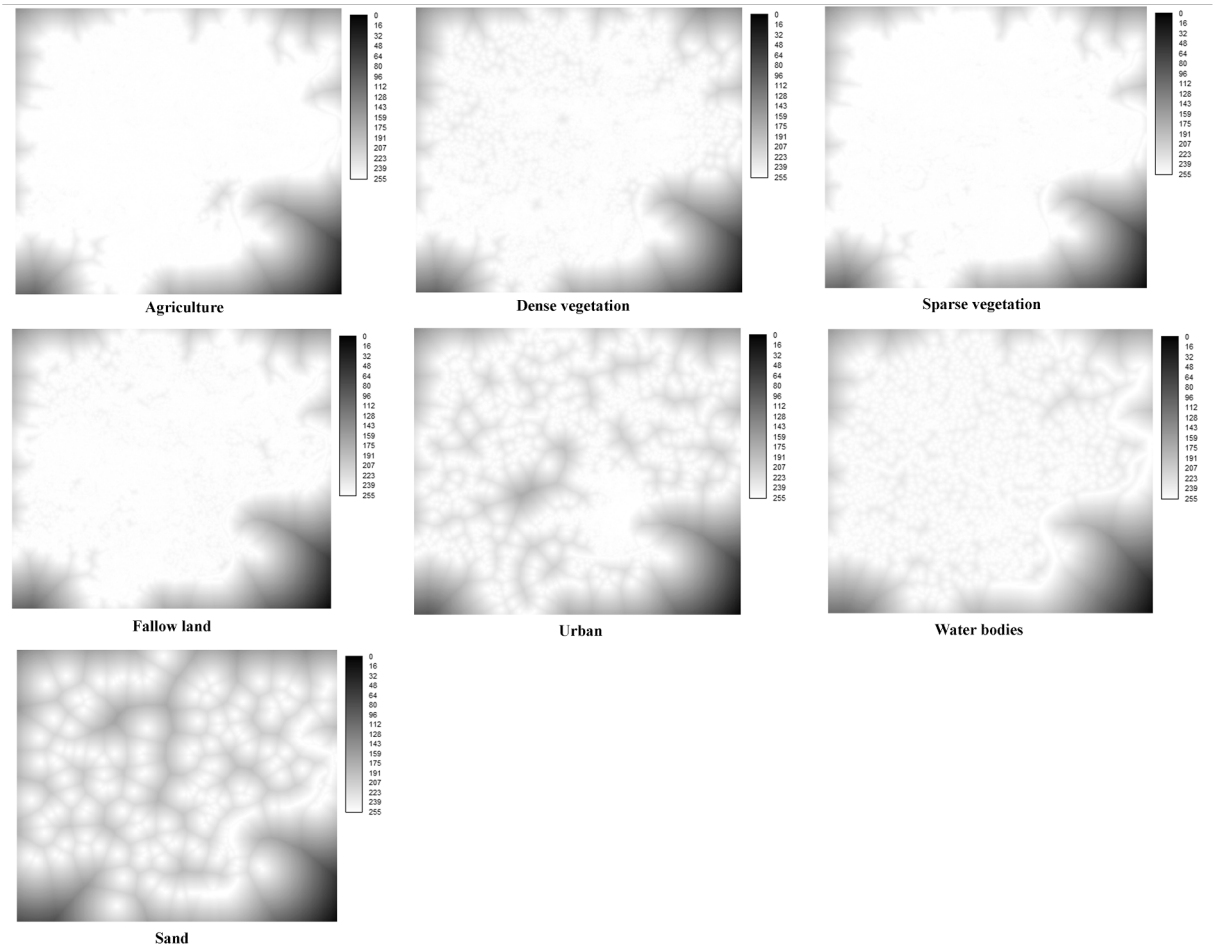

Fig. 4. Suitability maps for individual LULC categories.

4.2. LULCC analysis

In this study, the LULCC was quantified during the periods 1988–2001, 2001–2015, and 1988–2015 respectively. The changes in LULC were investigated by gains and losses occurred in different landscape categories (Fig. 7).

4.3. Evaluation of simulation models using landscape metrics

Different landscape metrics were derived using the simulated and the reference LULC maps to provide information on changing pattern of landscape and its configuration.

4.3.1. Performance evaluation based on metrics at class level

The simulated LULC classes of the year 2015 based on three land change models, namely ST_Markov, CA_Markov, and MLP_Markov are shown in Fig. 8(a, b, and c).

Differences between simulated maps of the year 2015 based on three land change models and a reference map of the year 2015 regarding the spatial arrangement of LULC types are shown in Figs. 9, 10, and 11 respectively.

The negative (underestimated) and positive (overestimated) RE values were found for every landscape metric of LULC types. The comprehensive description of the RE values for the calibrated ST_Markov simulation model is shown in Tables 6, 7 and 8.

Regarding the NP metric, the simulation model generated overestimated RE results for sparse vegetation, urban, water bodies and sand classes (46.05, 48.24, 51.83 and 88.93%, correspondingly) and in contrast, underestimated RE values for agriculture, dense vegetation and fallow land classes (−40.10, −43.28 and −54.90% respectively). By comparing the simulated and reference maps, agriculture and dense vegetation classes signified average, sparse vegetation, urban, water bodies, fallow land and sand represented low rank of agreement. In case of the AREA_MN metric, this model produced overestimated RE results for dense vegetation, water bodies, and sparse vegetation (60.27, 54.44, and 45.78%, respectively) and in contrast underestimated RE values for agriculture, fallow land, urban, and sand (-45.52, −37.39, −39.03 and − 52.39% respectively). The agreement level between the simulated and reference maps data are found to be average (fallow land, urban), and low (sparse vegetation, agriculture, dense vegetation, sand, and water bodies) respectively. For CA metric, the model generated the overestimated RE results for sand, sparse vegetation, urban, water bodies, and dense vegetation (83.93, 93.38, 95.32, 122.78, 139.75%, respectively) and in contrast underestimated RE values for agriculture and fallow land (−47.17, −43.82 respectively). The level of agreement between the simulated and reference map data are found to be average (fallow land), and low (sparse vegetation, dense vegetation, agriculture, urban, water bodies and sand) respectively. For ED metric, there is overestimated RE results for dense vegetation, urban, and water bodies (55.47, 50.28, and 59.99%, respectively) and in contrast underestimated RE values for agriculture, sparse vegetation, fallow land, and sand (−55.33, −45.33, and 30.98% respectively). The rank of agreement between the simulated and reference layers are found to be average (sand), and low (sparse vegetation, dense vegetation, agriculture, fallow land, urban, and water bodies) respectively. Comparing the simulated and reference maps, sand class showed average agriculture, fallow land, sparse vegetation, dense vegetation, urban, and water bodies represented low level of agreement. In case of ENN_MN metric, the model

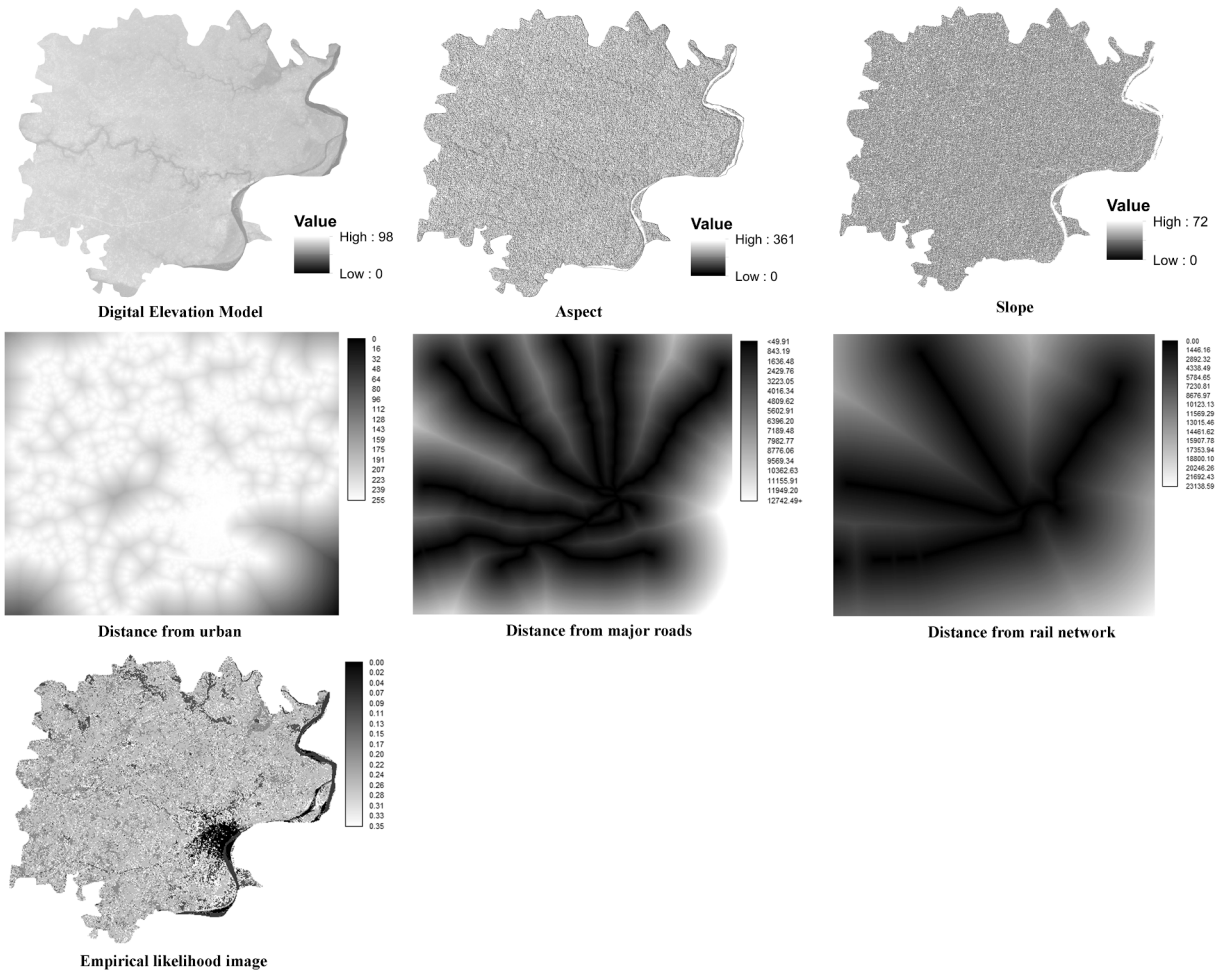

Fig. 5. Explanatory variables used in the study.

Table 5
Proposed relative error categorization scheme for evaluating the performance of simulation models.

Absolute RE (%)	Measure of agreement (between the simulated and reference layers)	Model performance
0–15	High	Excellent
15–30	Good	Good
30–45	Average	Moderate
> 45	Low	Weak

created overestimated RE values for agriculture and sparse vegetation (49.89 and 55.40%, correspondingly) and in contrast underestimated RE values for dense vegetation, fallow land, urban, water bodies and sand (−47.28, −40.41, −47.18, −42.79 and −45.90% respectively). The fallow land, water bodies, and sand represented average while agriculture, dense vegetation, sparse vegetation, and urban classes showed low rank of agreement between simulated and reference maps. In terms of LPI metric, this model produced overestimated RE values for agriculture, fallow land, and water bodies (43.21, 59.17, and 64.46%, respectively) while underestimated RE values for sparse vegetation, urban, dense vegetation, and sand categories (−36.82, −42.46, −50.04, and 53.16% respectively). The agreement level between the simulated and reference maps are found to be average (agriculture, sparse vegetation, and urban), and low (dense vegetation, fallow land, water bodies, and sand) respectively. For LSI metric, there are overestimated RE results for fallow land, urban, water bodies, and sand (49.96, 62.48, 56.64 and 57.37%, respectively) and in contrast underestimated RE values for agriculture, dense vegetation, and sparse vegetation (−47.13, −38.83, and 43.37% respectively). The dense vegetation and sparse vegetation showed average, while agriculture, fallow land, urban, water bodies, and sand represented low level of agreement between the simulated and reference maps. The ST_Markov simulation model performance was found to be high for ENN_MN and low for CA metrics respectively in terms of all LULC types. The detailed description of MRE values are given in Table 6. The MRE value was measured to be 55.36%, derived from class level metrics reflecting low model performance.

The comprehensive description of the RE values for the calibrated CA_Markov simulation model is shown in Tables 9, 10 and 11.

In case of the NP metric, there are considerable overestimated RE values for sparse vegetation, water bodies, fallow land, and sand classes (32.21, 32.61, 33.03, and 43.51%, respectively) and conversely underestimated RE values for urban, agriculture, and dense vegetation categories classes (−18.73, −25.88, and −31.34% respectively). The agriculture and urban represented good, fallow land, sparse vegetation, dense vegetation, water bodies and sand classes showed average agreement level by comparing the simulated and reference outputs. For the AREA_MN metric, the model generated overestimated RE values for dense vegetation, urban, and water bodies (33.40, 22.25, and 41.95%, respectively) and on other side there are underestimated RE values for agriculture, sparse vegetation, fallow land, and sand classes (−36.48, −26.57, −37.90 and −45.149% respectively). The level of agreement between the simulated and reference data are found good for sparse vegetation and urban, average for agriculture, dense vegetation, water bodies, and fallow land and low for sand. Regarding the CA metric, the model produced overestimated RE values for agriculture, dense

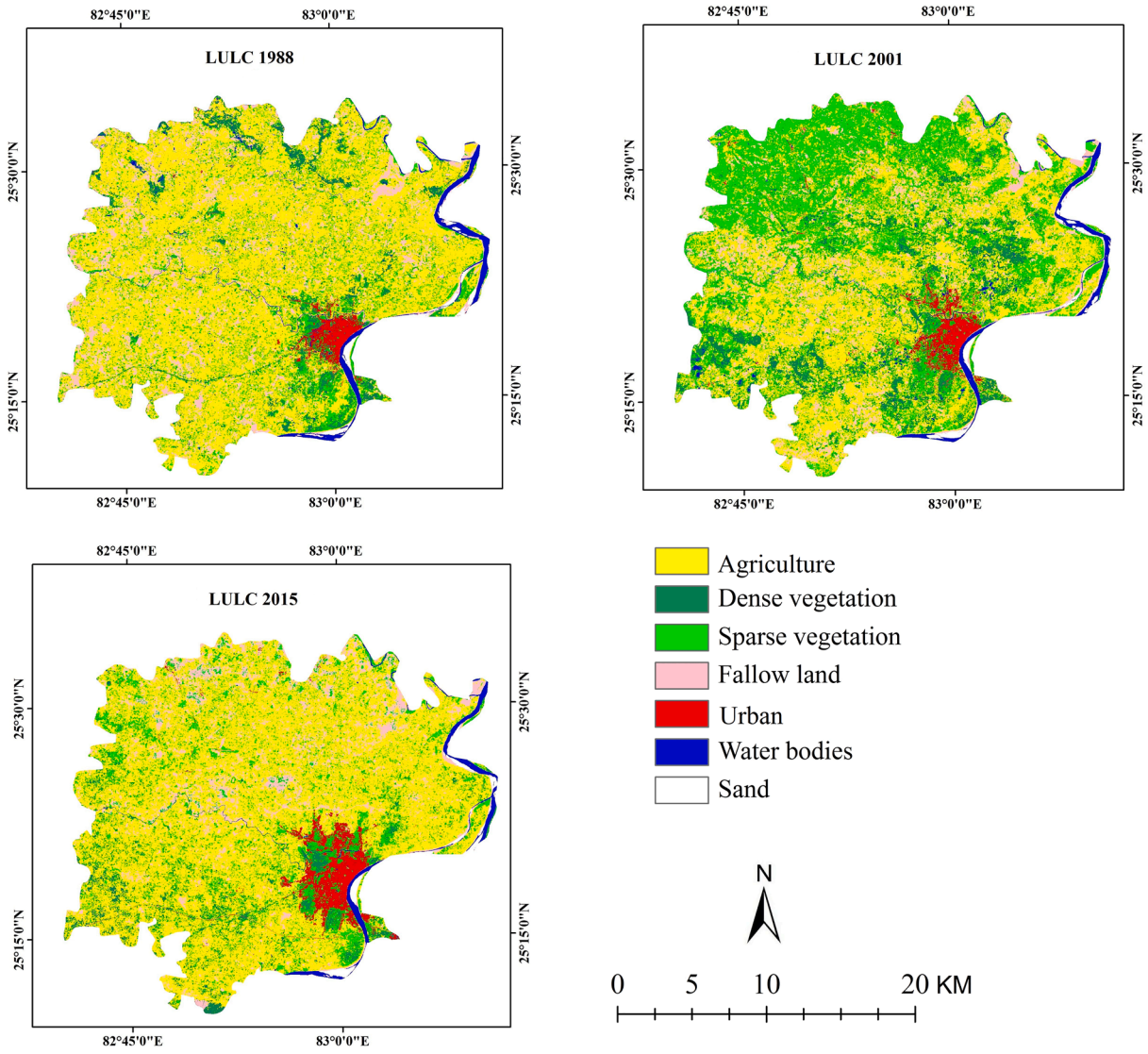

Fig. 6. Classified LULC maps of the study area.

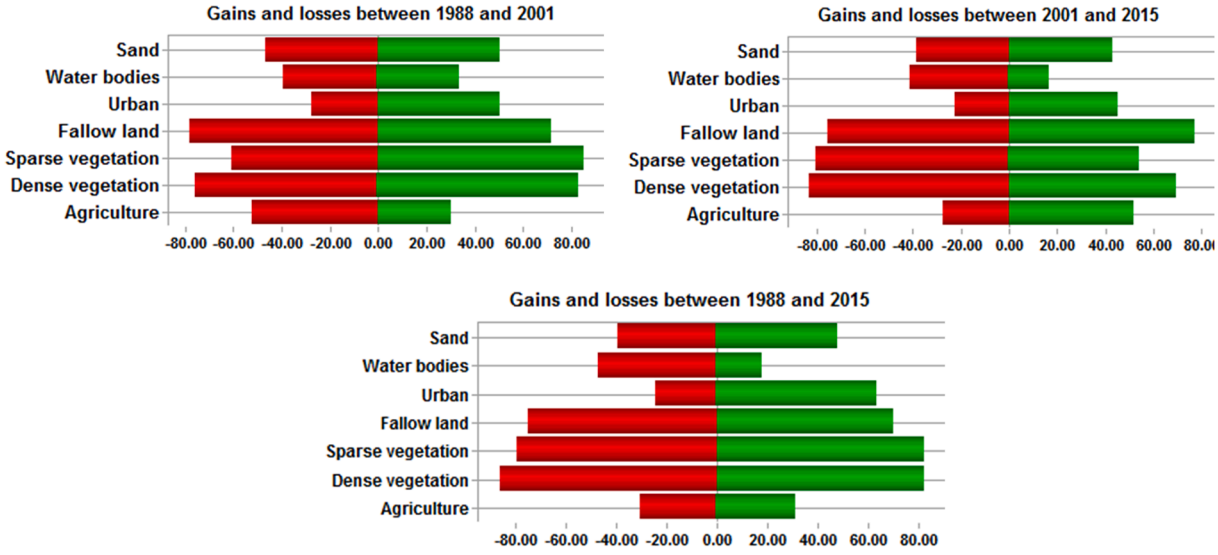

Fig. 7. Gains and losses in various LULC categories.

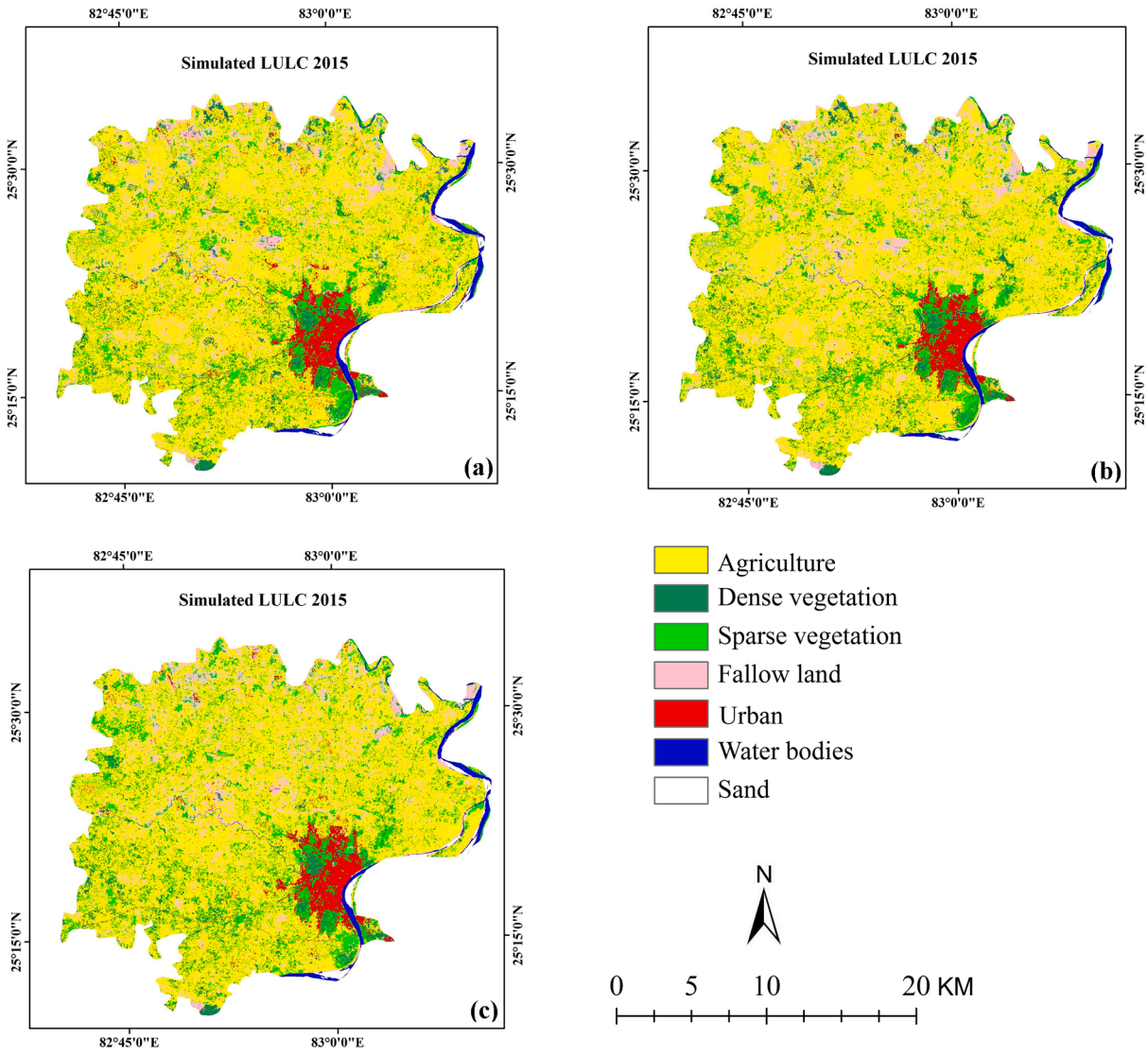

Fig. 8. Simulated LULC classes of the study area based on (a) ST_Markov; (b) CA_Markov; and (c) MLP_Markov models.

vegetation, fallow land, and water bodies (44.04, 40.26, 47.37, and 49.14%, respectively) and on the other side underestimated RE values for sparse vegetation, urban, and sand (−46.52, −32.84, and −51.89% respectively). Comparing the simulated and reference outputs, agriculture, dense vegetation, and urban categories represented average, fallow land, water bodies, sparse vegetation, and sand represented low level of agreement. For the ED metric, there are significant overestimated RE results for dense vegetation, fallow land, and water bodies (29.33, 54.21, and 48.48%, respectively) and conversely underestimated RE values for agriculture, sparse vegetation, urban, and sand (−33.10, −36.40, −41.74, and −49.02% respectively). The agreement rank between the simulated and reference maps are good for dense vegetation, average for agriculture, sparse vegetation, and urban, and low for water bodies, and sand classes. In terms of the ENN_MN metric, the model produced overestimated RE values for sparse vegetation and urban (52.05 and 39.91%, respectively), and in contrast underestimated RE values for agriculture, dense vegetation, fallow land, water bodies and sand (−23.22, −38.49, −46.80, −31.60 and −46.15% respectively). The agriculture represented good, dense vegetation, water bodies, and urban showed average, and sparse vegetation, fallow land, and sand classes demonstrated low agreement level between simulated and reference maps. In case of LPI metric, the model produced overestimated RE results for agriculture, dense vegetation, fallow land, and water bodies (37.39, 46.78, 48.85 and 49.53%, respectively) and in contrast there are underestimated RE values for sparse vegetation, urban, and sand (−46.03, −29.49, and −45.38% respectively). The agreement level between the simulated and reference map data are found to be good (urban), average (agriculture), and low (fallow land, sparse vegetation, dense vegetation, water bodies, and sand) respectively. In case of LSI metric, the model produced overestimated RE results for fallow land, and water bodies (42.59 and 48.46%, respectively) and contrary underestimated RE values for agriculture, dense vegetation, sparse vegetation, urban, and sand (−40.34, −34.08, 29.85, 46.73 and 51.81% respectively). The agreement level between the simulated and reference map data are found to be good (sparse vegetation), average (agriculture, dense vegetation and fallow land), and low (urban, water bodies, and sand) respectively. The CA_Markov model performance was found to be high and low for NP and CA metrics, respectively for all LULC categories. The MRE values were found to be highest (31.04%) and lowest (46.98%) for CA and ENN_MN metrics respectively. The detailed description of MRE values are represented in Table 9. The MRE value was measured to be 39.61%, derived from class level metrics reflecting average model performance. The comprehensive description of the RE values of the calibrated MLP_Markov simulation model is shown in Tables 12, 13 and 14.

The NP metric depicted a substantial difference between simulation

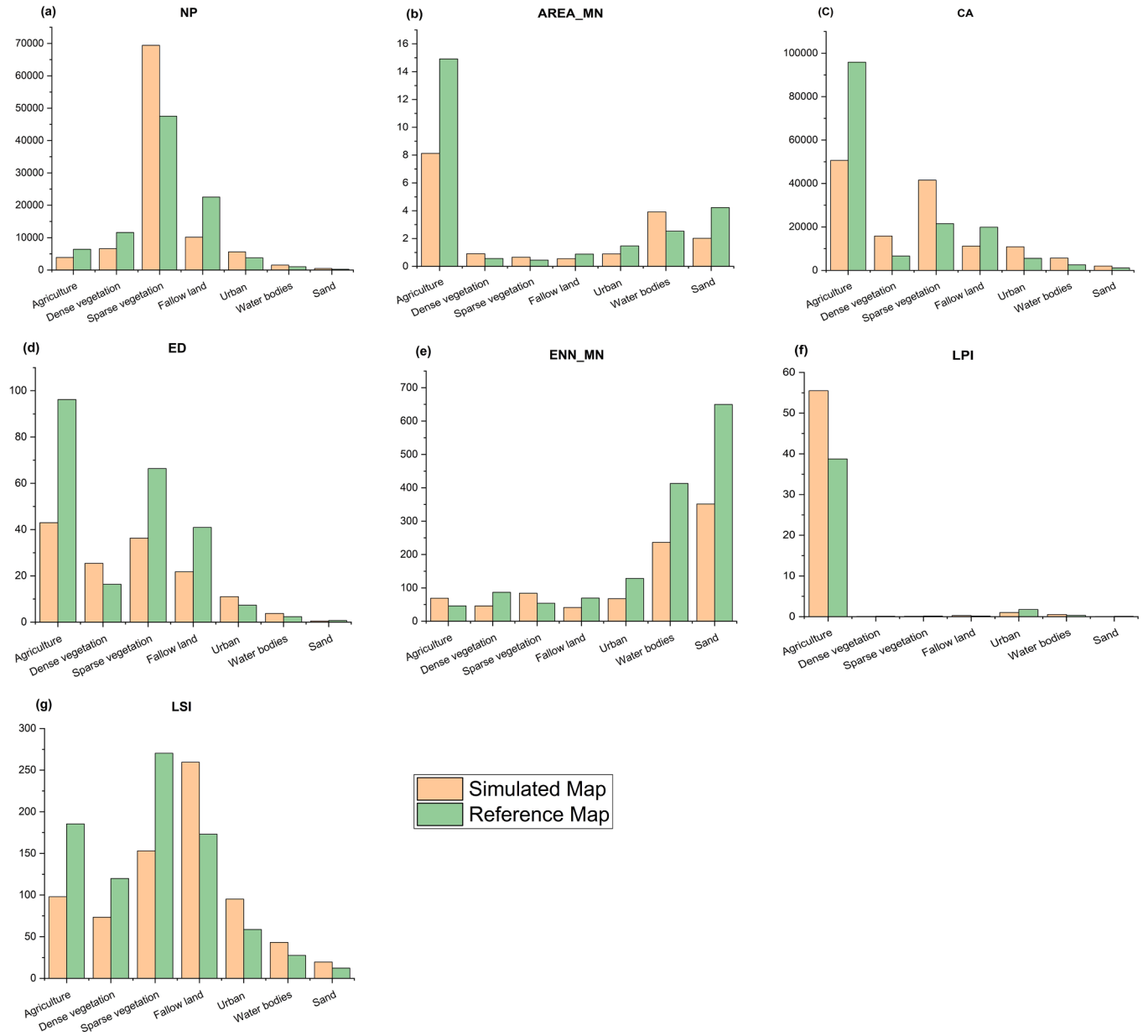

Fig. 9. Differences between the ST_Markov based simulated and reference LULC categories.

and reference layers in terms of RE values. The simulation model tends to overestimate RE values for fallow land, urban, and sand classes (33.63, 13.30, and 40.08% respectively), conversely, there are underestimated RE values results for water bodies, sparse vegetation, dense vegetation, and agriculture (−35.68, −27.62, –22.52, and −16.79% respectively). The degree of similarity related to NP metric for sand, water bodies, fallow land, sparse vegetation, dense vegetation, agriculture, and urban categories are average, average, average, good, good, and high respectively. For AREA_MN metric, the simulation model represented overestimated outcomes for agriculture, dense vegetation, sparse vegetation, and water bodies having RE values of 13.87, 14.60, 19.27, and 33.03%, respectively. In contrary, fallow land, urban, and sand classes showed underestimated results (RE = − 25.37, −10.91, −33.77 respectively). Considering AREA_MN metric, the agreement level between the simulated and reference map data is found to be high (agriculture, dense vegetation and urban), good (fallow land and sparse vegetation), and average (sand and water bodies), respectively. Regarding the CA metric, there are substantial overestimated values for agriculture, urban and water bodies, which demonstrated 12.59, 17.71, and 22.99% of RE values respectively, conversely, there are underestimated results for sparse vegetation, sand, fallow land, and dense vegetation with RE values of −29.66, −25.65, −20.84, and −18.08% respectively. The simulated and reference layers show high (agriculture), and good (urban, fallow land, sparse vegetation, dense vegetation, water bodies and sand) level of agreement. For the ED metric, there are overestimated results for urban, water bodies, and sand categories (RE = 11.83, 26.26, and 28.61%, respectively). Agriculture, dense vegetation, sparse vegetation, and fallow land categories depicted underestimated RE values (−15.33, −17.48, −13.04, and –22.61% respectively). The level of agreement is high for sparse vegetation and urban, and good for agriculture, dense vegetation, water bodies, fallow land and sand categories by comparing simulated and reference layers. In case of the ENN_MN metric, there are a significant overestimated RE value for sparse vegetation class demonstrating 18.94%, followed by dense vegetation category (RE = 13.26%) Conversely, there are underestimated results for agriculture, fallow land, urban, water bodies and sand categories with RE values of −17.55, −16.68, −15.00, –23.81 and −38.01% respectively. The degree of similarity concerning

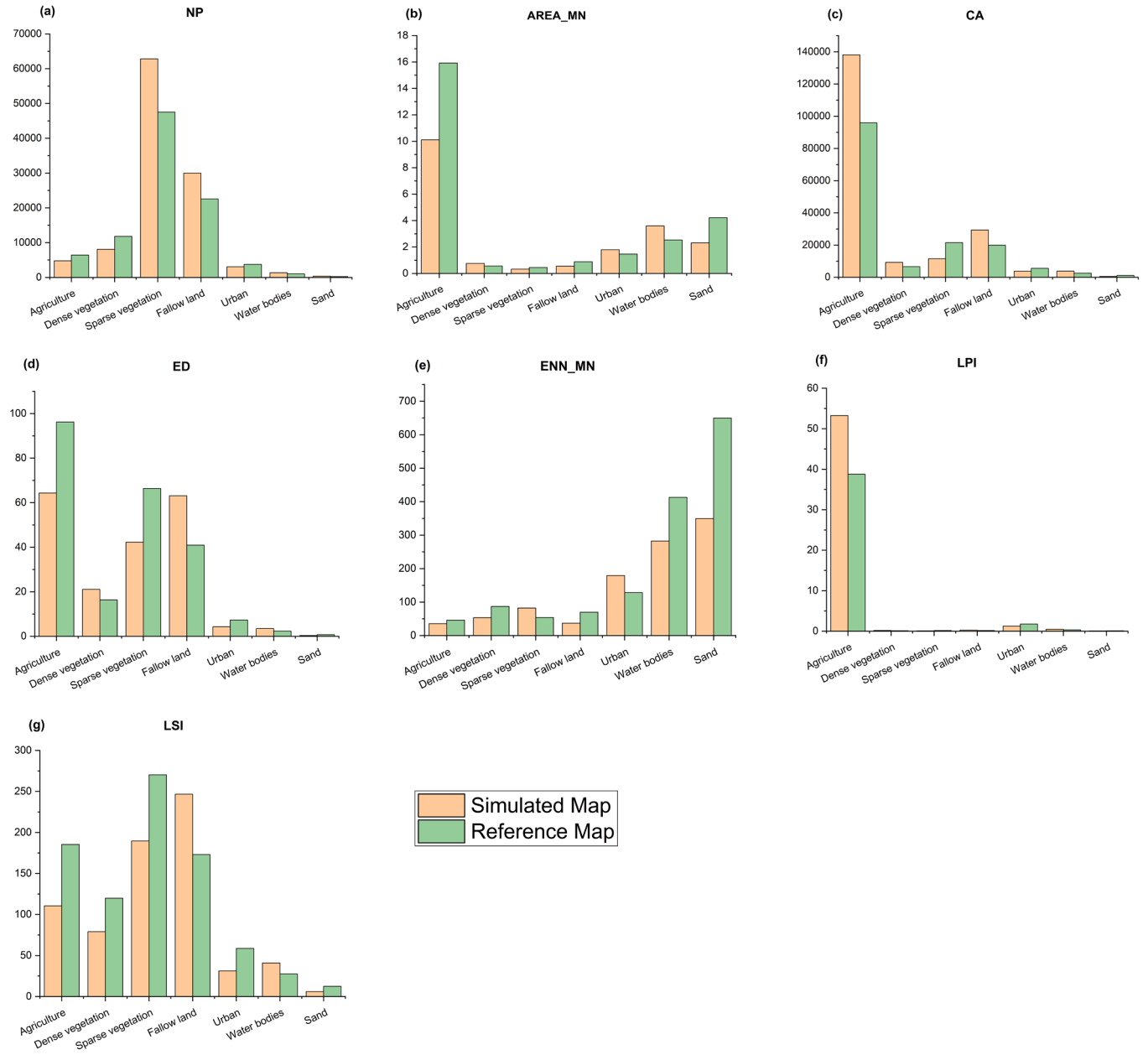

Fig. 10. Differences between the CA_Markov based simulated and reference LULC categories.

ENN_MN metric for sand, water bodies, urban, fallow land, sparse vegetation, agriculture, dense vegetation are average, good, good, good, good, good, and high correspondingly. In terms of the LPI metric, simulation model depicted overestimated results for dense vegetation, fallow land, agriculture, sparse vegetation, and water bodies 16.90, 18.76, 19.22, 20.40, and 30.53%, respectively. In contrary, there are underestimated values for urban and sand classes (RE = −15.30 and −26.53% respectively). Considering LPI metric, the agreement level between simulated and reference layers was evaluated as good (agriculture, fallow land, sparse vegetation, dense vegetation, urban, and sand), and average (water bodies), respectively. For the LSI metric, the model generates overestimated RE results for fallow land, urban, water bodies, and sand (25.89, 19.32, 24.97 and 21.86%, respectively) and in contrast there are underestimated RE values for agriculture, dense vegetation, sparse vegetation (−14.71, −15.28, and –23.59% respectively). Comparing the simulated and reference layers, urban category depicted high, agriculture, fallow land, sparse vegetation, dense vegetation, water bodies categories represented good and sand showed average level of agreement. The MLP_Markov model illustrated high performance for ED metric and low for NP metric in terms of all LULC types. The MRE values were found to be highest (19.31%) and lowest (27.09%) for ED and NP metrics respectively. The MRE value was measured to be 21.63%, derived from class level metrics that reflect good model performance. The detailed report of MRE values are demonstrated in Table 12.

4.3.2. *Performance evaluation based on metrics at the landscape level*

Fig. 9 and Table 15 show the discrepancy at the landscape level, between the measured metrics and RE values for the outcomes of ST_Markov simulation model, mentioning to the simulated and reference maps. The ENN_MN metric showed the maximum variation between the results of the model and resultant classes in the reference layer (RE value underestimated as − 47.50%). Alternatively, the AREA_MN metric showed the minimum variation with the RE value of 44.31% difference from its true value. The average agreement was observed between the simulated and reference maps for NP, AREA_MN and ED

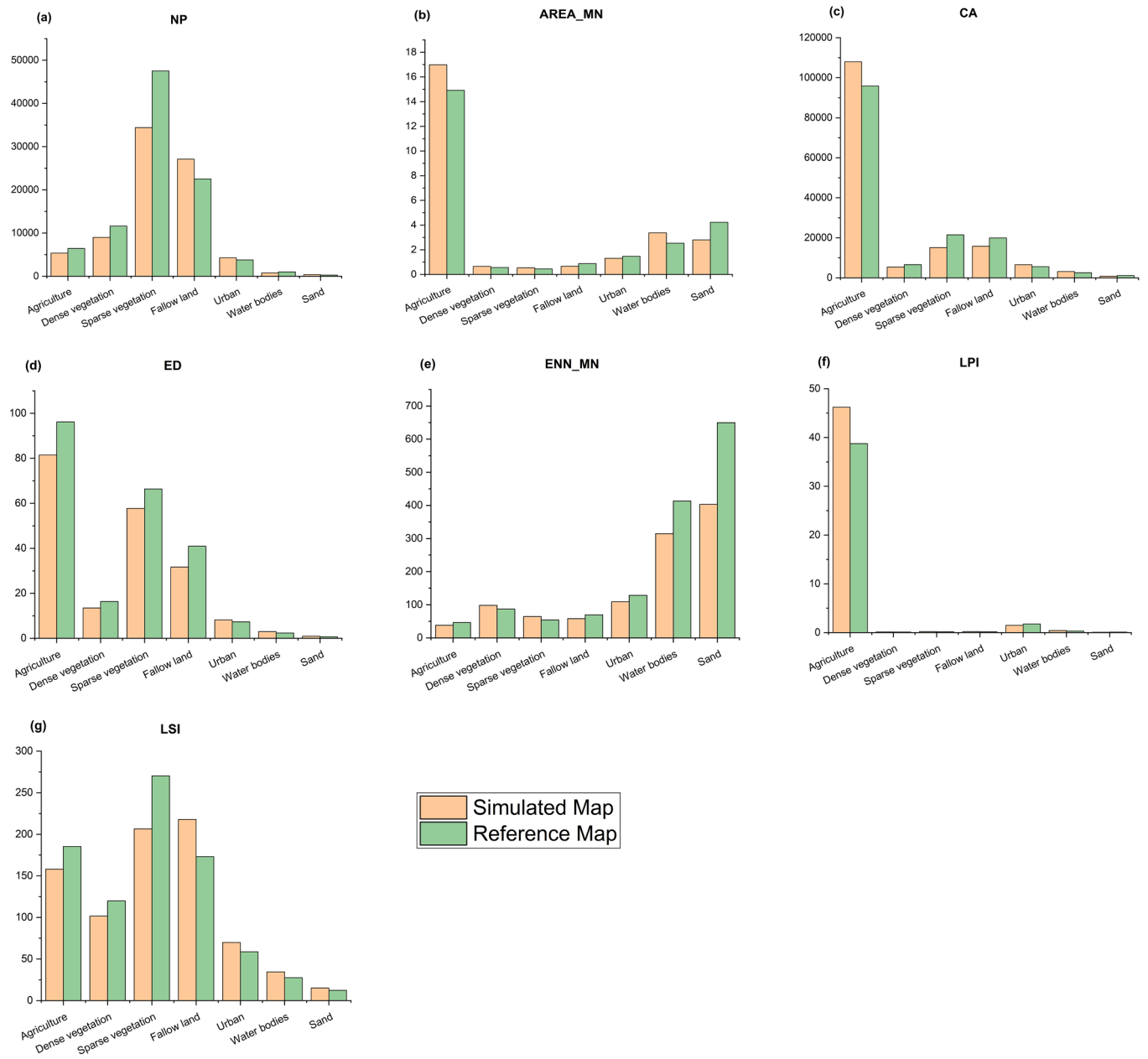

Fig. 11. Differences between the MLP_Markov based simulated and reference LULC categories.

Table 6
The values of RE and MRE for each LULC types and landscape metric at class level using ST_Markov simulation model.

LULC type/ Landscape metric	NP	Area_MN	CA	ED	ENN_MN	LPI	LSI	MRE_{LULC} (%)
Agriculture	−40.10	−45.52	−47.17	−55.33	49.89	43.21	−47.13	46.91
Dense vegetation	−43.28	60.27	139.75	55.47	−47.28	−50.04	−38.83	62.13
Sparse vegetation	46.05	45.78	93.38	−45.33	55.40	−36.82	−43.37	52.30
Fallow land	−54.90	−37.39	−43.82	−46.81	−40.41	59.17	49.96	47.49
Urban	48.24	−39.03	95.32	50.28	−47.18	−42.46	62.48	55.00
Water bodies	51.83	54.44	122.78	59.99	−42.79	64.46	56.64	64.70
Sand	88.93	−52.39	83.93	−30.98	−45.90	−53.16	57.37	58.95
MRE_{metric} (%)	53.33	47.83	89.45	49.17	46.98	49.90	50.83	55.36

metrics at the landscape level. The low agreement was observed between the simulated and reference maps for ENN_MN, LPI and LSI metrics at the landscape level. The MRE value was estimated to be 45.75% at the landscape level, showing the weak performance of the ST-MC simulation model.

Fig. 10 and Table 16 show the variations at the landscape level, between the measured metrics and RE values for CA_Markov model outcomes, mentioning to the simulated and reference maps. The LSI metric showed the maximum deviation between model results and resultant classes in the reference map having underestimated value of

Table 7
Rank of agreement at class level between the simulated and reference LULC maps using ST_Markov simulation model.

LULC type/ Landscape metric	NP	Area_MN	CA	ED	ENN_MN	LPI	LSI
Agriculture	Average	Low	Low	Low	Low	Average	Low
Dense vegetation	Average	Low	Low	Low	Low	Low	Average
Sparse vegetation	Low	Low	Low	Low	Low	Average	Average
Fallow land	Low	Average	Average	Low	Average	Low	Low
Urban	Low	Average	Low	Low	Low	Average	Low
Water bodies	Low	Low	Low	Low	Average	Low	Low
Sand	Low	Low	Low	Average	Average	Low	Low
$Agreement_{metric}$	Low	Low	Low	Low	Low	Low	Low

Table 8
Rank of the performance of ST_Markov simulation model for all LULC types and calculated landscape metrics at class level.

LULC type/ Landscape metric	NP	Area_MN	CA	ED	ENN_MN	LPI	LSI
Agriculture	Moderate	Weak	Weak	Weak	Weak	Moderate	Weak
Dense vegetation	Moderate	Weak	Weak	Weak	Weak	Weak	Moderate
Sparse vegetation	Weak	Weak	Weak	Weak	Weak	Moderate	Moderate
Fallow land	Weak	Moderate	Moderate	Weak	Moderate	Weak	Weak
Urban	Weak	Moderate	Weak	Weak	Weak	Moderate	Weak
Water bodies	Weak	Weak	Weak	Weak	Average	Weak	Weak
Sand	Weak	Weak	Weak	Weak	Average	Weak	Weak
Model $performance_{metric}$	Weak	Weak	Weak	Weak	Weak	Weak	Weak

Table 9
The values of RE and MRE for each LULC types and landscape metric at class level using CA_Markov simulation model.

LULC type/ Landscape metric	NP	Area_MN	CA	ED	ENN_MN	LPI	LSI	MRE_{LULC} (%)
Agriculture	−25.88	−36.48	44.04	–33.10	–23.22	37.39	−40.34	34.35
Dense vegetation	−31.34	33.40	40.26	29.33	−38.49	46.78	−34.08	36.24
Sparse vegetation	32.21	−26.57	−46.52	−36.40	52.05	−46.03	−29.85	38.52
Fallow land	33.03	−37.90	47.37	54.21	−46.80	48.85	42.59	44.39
Urban	−18.73	22.25	–32.84	−41.74	39.91	−29.49	−46.73	33.10
Water bodies	32.61	41.95	49.14	48.48	−31.60	49.53	48.46	43.11
Sand	43.51	−45.14	−51.89	−49.02	−46.15	−45.38	−51.81	47.56
MRE_{metric} (%)	31.04	34.81	44.58	41.75	39.75	43.35	41.98	39.61

Table 10
Rank of agreement at class level between the simulated and reference LULC maps using CA_Markov simulation model.

LULC type/ Landscape metric	NP	Area_MN	CA	ED	ENN_MN	LPI	LSI
Agriculture	Good	Average	Average	Average	Good	Average	Average
Dense vegetation	Average	Average	Average	Good	Average	Low	Average
Sparse vegetation	Average	Good	Low	Average	Low	Low	Good
Fallow land	Average	Average	Low	Low	Low	Low	Average
Urban	Good	Good	Average	Average	Average	Good	Low
Water bodies	Average	Average	Low	Low	Average	Low	Low
Sand	Average	Low	Low	Low	Low	Low	Low
$Agreement_{metric}$	Average	Average	Average	Average	Average	Average	Average

Table 11
Rank of the performance of CA_Markov simulation model for all LULC types and calculated landscape metrics at class level.

LULC type/ Landscape metric	NP	Area_MN	CA	ED	ENN_MN	LPI	LSI
Agriculture	Good	Moderate	Moderate	Moderate	Good	Moderate	Moderate
Dense vegetation	Moderate	Moderate	Moderate	Good	Moderate	Weak	Moderate
Sparse vegetation	Moderate	Good	Weak	Moderate	Weak	Weak	Good
Fallow land	Moderate	Moderate	Weak	Weak	Weak	Weak	Moderate
Urban	Good	Good	Moderate	Moderate	Moderate	Good	Weak
Water bodies	Moderate	Moderate	Weak	Weak	Moderate	Weak	Weak
Sand	Moderate	Weak	Weak	Weak	Weak	Weak	Weak
Model $performance_{metric}$	Moderate	Moderate	Moderate	Moderate	Moderate	Moderate	Moderate

RE is − 36.97%. Alternatively, the AREA_MN metric showed the minimum variation with the RE value of 20.98% difference from its actual value. A good agreement was observed between the simulated and reference maps for NP, AREA_MN, and ED metrics at the landscape level. The average agreement was observed between the simulated and reference maps for ENN_MN, LPI, and LSI metrics at the landscape level. The MRE value was estimated to be 28.31% at the landscape level, showing the good performance of the CA_Markov simulation model.

Table 12
The values of RE and MRE for each LULC types and landscape metric at class level using MLP_Markov simulation model.

LULC type/ Landscape metric	NP	Area_MN	CA	ED	ENN_MN	LPI	LSI	MRE_{LULC} (%)
Agriculture	−16.79	13.87	12.59	−15.33	−17.55	19.22	−14.71	15.72
Dense vegetation	–22.52	14.60	−18.08	−17.48	13.26	16.90	−15.28	16.88
Sparse vegetation	−27.62	19.27	−29.66	−13.04	18.94	20.40	–23.59	21.79
Fallow land	33.63	−25.37	−20.84	–22.61	−16.68	18.76	25.89	23.40
Urban	13.30	−10.91	17.71	11.83	−15.00	−15.30	19.32	14.77
Water bodies	−35.68	33.03	22.99	26.26	–23.81	30.53	24.97	28.18
Sand	40.08	–33.77	−25.65	28.61	−38.01	−26.53	21.86	30.64
MRE_{metric} (%)	27.09	21.55	21.07	19.31	20.46	21.09	20.80	**21.63**

Table 13
Rank of agreement at class level between the simulated and reference LULC maps using MLP_Markov simulation model.

LULC type/ Landscape metric	NP	Area_MN	CA	ED	ENN_MN	LPI	LSI
Agriculture	Good	High	High	Good	Good	Good	Good
Dense vegetation	Good	High	Good	Good	High	Good	Good
Sparse vegetation	Good	Good	Good	High	Good	Good	Good
Fallow land	Average	Good	Good	Good	Good	Good	Good
Urban	High	High	Good	High	Good	Good	High
Water bodies	Average	Average	Good	Good	Good	Average	Good
Sand	Average	Average	Good	Good	Average	Good	Average
$Agreement_{metric}$	Good	Good	Good	Good	Good	Good	Good

Table 14
Rank of the performance of MLP_Markov simulation model for all LULC types and calculated landscape metrics at class level.

LULC type/ Landscape metric	NP	Area_MN	CA	ED	ENN_MN	LPI	LSI
Agriculture	Good	Excellent	Excellent	Good	Good	Good	Good
Dense vegetation	Good	Excellent	Good	Good	Excellent	Good	Good
Sparse vegetation	Good	Good	Good	Excellent	Good	Good	Good
Fallow land	Moderate	Good	Good	Good	Good	Good	Good
Urban	Excellent	Excellent	Good	Excellent	Good	Good	Excellent
Water bodies	Moderate	Moderate	Good	Good	Good	Moderate	Good
Sand	Moderate	Moderate	Good	Good	Moderate	Good	Moderate
Model $performance_{metric}$	Good	Good	Good	Good	Good	Good	Good

Table 15
Metrics value, RE, MRE of ST_Markov simulation model results and landscape level agreement for reference and simulated LULC maps.

Metric/value	NP	AREA_MN	ED	ENN_MN	LPI	LSI	$MRE_{landscape\ level}$
Reference layer	93,139	2.5631	115.7812	69.9383	38.7582	142.4188	
Simulated layer	56,457	3.6988	66.105	36.7205	59.5042	75.6857	
Relative error	−39.38	44.31	−42.91	−47.50	53.53	−46.86	45.75
Level of agreement	Average	Average	Average	Low	Low	Low	
Model performance	Moderate	Moderate	Moderate	Weak	Weak	Weak	Weak

Table 16
Metrics value, RE, MRE of CA_Markov simulation model results and landscape level agreement for reference and simulated LULC maps.

Metric/value	NP	AREA_MN	ED	ENN_MN	LPI	LSI	$MRE_{landscape\ level}$
Reference layer	93,139	2.5631	115.7812	69.9383	38.7582	142.4188	
Simulated layer	70,889	3.1008	86.0104	48.9125	26.2508	89.7626	
Relative error	–23.89	20.98	−25.71	−30.06	–32.27	−36.97	28.31
Level of agreement	Good	Good	Good	Average	Average	Average	
Model performance	Good	Good	Good	Moderate	Moderate	Moderate	Good

Table 17
Metrics value, RE, MRE of MLP_Markov simulation model results and landscape level agreement for reference and simulated LULC maps.

Metric/value	NP	AREA_MN	ED	ENN_MN	LPI	LSI	$MRE_{landscape\ level}$
Reference layer	93,139	2.5631	115.7812	69.9383	38.7582	142.4188	
Simulated layer	80,756	2.9324	99.131	76.8525	44.4378	123.126	
Relative error	−13.30	14.41	−14.38	9.89	14.65	−13.55	11.45
Level of agreement	High	High	High	High	High	High	
Model performance	Excellent	Excellent	Excellent	Excellent	Excellent	Excellent	Excellent

Fig. 11 and Table 17 show the differences between the metrics and RE values measured at the landscape level for MLP_Markov model outcomes, mentioning the simulated and reference maps. The LSI metric showed the maximum deviation between model results and resultant classes in the reference data with the underestimated RE value of −13.55%. Alternatively, the ENN_MN metric showed the minimum variation having RE value of 9.89% from its actual value. A good agreement was observed between the simulated and reference maps for NP, AREA_MN, and ED metrics at the landscape level. The high agreement was observed between the simulated and reference maps for all the landscape level metrics. The MRE value was estimated to be 11.45% at the landscape level, showing excellent performance of the MLP-MC simulation model.

5. Discussion

The success and performance of simulation models merely based on quantity are unable to deliver information to the researchers with respect to spatial metrics and morphological features. For that, the spatially-explicit scheme is required to evaluate the performance of the spatially-explicit predictive models. In addition, this scheme is expected to provide information on model behavior. Hence this work proposed an advanced method based on the study of landscape pattern, for evaluating the performance of the model. The proposed methodology exhibits a unique feature of landscape metrics in terms of its spatial composition that leads to the hierarchical and multi-level study of the performance of scenario-based spatial models. It also consented to quantify the success of the simulation process concerning the structure and patterns of landscape. The significant differences have also been illustrated between the performance of models at class and landscape levels. In the case of the MLP_Markov simulation model, the resultant MRE values are 21.63% and 11.45% at class and landscape-level respectively. The final MRE value was 11.45% at the landscape level. This vital outcome demonstrated a source of synchronized investigation of model performance at various levels. It may also be explicated with the help of calculation method and incorporation of supplementary information to investigate landscape pattern at the class level. The performance of MLP_Markov simulation model as per the results was found to be the best in comparison to other models used in this study. The performance of MLP_Markov model was high for urban class, good for sparse vegetation, and the average for sand at the class level. The performance of the MLP-MC simulation model was found to be excellent for all the metrics at the landscape level.

The success of the MLP_Markov simulation model can be described as follows:

1) During the simulation process, there is a trend of having higher NP for agriculture, sparse vegetation, dense vegetation and water bodies. Lower NP for fallow land, urban and sand categories.
2) In the simulated maps, the shape of patches shown by LSI became simpler and larger in size for agriculture, sparse vegetation, and dense vegetation. Whereas smaller in size for fallow land, urban, water bodies and sand categories.
3) Putting together the above-mentioned points, the model results are facile in opposition to the spatial pattern derived from actual LULC maps.
4) Based on Tables 12 and 17, the performance of MLP_Markov simulation model at the landscape level was found to be excellent in comparison to that of class level having good results.
5) It is revealed that MLP_Markov model implemented well in the spatial simulation of LULC categories on the basis of an inclusive deliberation of the outcomes

According to McGarigal et al. (2002) there is the availability of several measures at class and landscape levels which is vital to get an empirical relationship among these indices (CA, NP, Area_MN, ED, ENN_MN, LSI, and LPI) to develop a ~~valuable~~ better combination for evaluating the performance of simulation models. Therefore, it is useful to pick the nominal and more reliable set of metrics to recognize a set of structural elements that jointly depict key independent features of landscape successfully (Cushman et al., 2008). This study showed the effectiveness of various indices to discriminate the model performance at class and landscape levels. The patch size, shape and neighborhood of a LULC class characterize the model performance at the class level. An overall landscape heterogeneity, texture, is used to illustrate the success of the simulation model at the landscape level (Cushman et al., 2008). This type of analysis at class-level is of significance to distinguish between composition and pattern due to its conceptually diverse aspect of the landscape configuration (Fahrig, 2002). It is important to note that the selection of associated matrices might raise redundancy and generate overstated outcomes. Conversely, the omission of appropriate metrics will lead to the dimensionality reduction of landscape constitution (Cushman et al., 2008). The behavior of landscape and research problems would be the basis for the selection of matrices. The metrics used in this study would not be adequate to incarcerate the complete characteristics of a specific study site. It is quite feasible that these universally attributed metrics might present consistently in other study regions. But still, the distinctive characteristics of a landscape structure may also require choosing particular metrics.

This study also assessed the comparative simulation capabilities of MLP_Markov, CA_Markov, and ST_Markov integrated models from an ecological point of view. The result of the study pointed out that the integration of Markov with MLP performed best among the three, followed by CA_Markov and ST_Markov models. This finding has significant ecological implications for both: terrestrial as well as aquatic ecosystems (Trombulak and Frissell, 2000) as the changes in LULC is connected to various aspects of ecosystems. For instance, in the terrestrial ecosystem, changes in forest cover over a period of time can be related to ‘concurrent species richness of bees and wasps’ as well as community composition which may lead to shift in pollinator community (Tan et al., 2020). Similarly, the changes in water bodies like stream, lake, pond surface areas also have ecological implications (Allan and Flecker, 1993). For example, alteration in “hydrologic regimes and potential biological responses” due to expansion in impervious structures including pucca roads, rural and urban settlements, etc. lead to changes in characteristics of benthic and pelagic species’ habitat. The ratio of benthic to pelagic planktonic diatoms to land use changes has also been found to be correlated (Liu et al., 2020). Hence, the better performance of LULC simulation can be used for ranking the ecological indices linking interconnectedness of LULC changes and various ecological parameters (Prasad et al., 2010).

The results procured through this study is found of very good accuracy, specifically for MLP_Markov model-based simulation on the focused region of interest. Having the same topography and geo-environmental condition of any region, this study can be a value addition work to conduct simulation-based research using utilized models. Further, the work can be compared with other models, especially ensemble based, to check the performance and accuracy of models and identification of better models among all on the present study area or on the other regions as well. The landscape metrics derived from thematic LULC maps are sensitive to geometric misregistration of inter-annual images and intrinsic uncertainties. The major sources of uncertainties are classification scheme, spatial scale, geometric misregistration, and classification error (Lechner et al., 2012). Additionally, inaccurate description of LULC classes is another cause of ambiguity in the classification method. The results of image classification will also be affected by different methods. In this study, moderate spatial resolution images of 30 m acquired from Landsat series satellites were used. These images were chosen because higher resolutions might needlessly add to data volume, and coarser resolutions can result in information loss. The resolution of thematic maps is dependent on the objectives and scale of the present work.

6. Conclusions

Since the ecological diversity and its resilience is under constant challenge due to immense influx of regional, national, and international population, the spatio-temporal changes in the landscape of Varanasi district were evaluated based on LULC data for the years 1988, 2001, and 2015. The current study implemented a machine learning and statistical ensembles entwined through a diverse procedure to appraise and compare the performance of MLP_Markov, CA_Markov and ST_Markov land change simulation models, which is revealed by metrics calculations based on consequential RE values. In addition, the consequences of the scenario description on model performance are assessed with the help of landscape metrics and it aids to novelty of this work. The performance of MLP_Markov model was found to be excellent with MRE value 11.45% at the landscape level. A comprehensive deliberation of the results of the integrated MLP_Markov model revealed its success in spatial simulation of landscape scenario. Assimilation of the driver variables supports as well to recognize the potential factors of LULC conversion during simulation process. This study highlighted that the urban expansion description from 1988 to 2001 is expected to persist as well in succeeding epoch (2001 to 2015) based on simulated results. A variety of metrics in different study areas can be used for selecting a most favorable and descriptive group of the metrics. So, there is also a possibility that other simulation models would oblige a diverse collection of metrics in different study regions.

However, the accuracy of the simulation results is strongly connected to several factors. Primarily, the accuracy of LULC layers is undesirably affected by the moderate spatial resolution of the Landsat images that may lead to influence the reliability of simulated results. So, the images from high resolution sensors would be beneficial in simulating more reliable landscape scenarios. The inclusion of random variables, like government policies, socio-economic aspects, and biophysical parameters is still a challenging task and hence, it needs to be explored in future studies. It is also of significant interest to explore the consequences of changing spatial scale on the performance of simulation models and their quantification through landscape metrics.

The results can be of interest for researchers attempting to explore the effects of changing structures on a particular landscape function and project more realistic future scenarios. The results of the present study can also be used as input in studies exploring the effect of LULC changing scenarios on floral and faunal biodiversity and the area's ecosystem resilience.

CRediT authorship contribution statement

Aman Arora: Software, Data curation, Formal analysis. **Manish Pandey:** Writing - original draft, Formal analysis, Visualization. **Varun Narayan Mishra:** Conceptualization, Methodology, Writing - review & editing. **Ritesh Kumar:** Formal analysis, Validation. **Praveen Kumar Rai:** Investigation, Validation. **Romulus Costache:** Formal analysis, Investigation. **Milap Punia:** Investigation. **Liping Di:** Investigation.

Declaration of Competing Interest

The authors declare that they have no known competing financial interests or personal relationships that could have appeared to influence the work reported in this paper.

Acknowledgements

The authors wish to gratefully acknowledge the United States Geological Survey (USGS) for providing Landsat data at no cost. The authors are also thankful to the editor and anonymous reviewers for their insightful comments which helped in improving the manuscript.

References

Aaviksoo, K., 1995. Simulating vegetation dynamics and land use in a mire landscape using a Markov model. Landsc. Urban Plan. 31 (1–3), 129–142.
Allan, J.D., Flecker, A.S., 1993. Biodiversity conservation in running waters. Bioscience 43, 32–43.
Amiri, B.J., Asgarian, A., Sakieh, Y., 2017. Introducing landscape accuracy metric for spatial performance evaluation of land use/land cover change models. Geocarto Int. 32 (11), 1171–1187.
Araya, Y.H., Cabral, P., 2010. Analysis and modeling of urban land cover change in Setúbal and Sesimbra, Portugal. Remote Sens. 2 (6), 1549–1563.
Arora, A., Pandey, M., Siddiqui, M.A., Hong, H., Mishra, V.N., 2019. Spatial flood susceptibility prediction in Middle Ganga Plain: comparison of frequency ratio and Shannon's Entropy models. Geocarto Int. https://doi.org/10.1080/10106049.2019.1687594.
Arora, A., Pandey, M., Singh, A., Siddiqui, M.A., 2018. Study of landscape evolution in North Koel River Basin, Jharkhand, India: tectonic and structural implications based on hypsometric analysis. Forum Geogra. 17 (2), 111–117.
Arsanjani, J.J., Helbich, M., Kainz, W., Boloorani, A.D., 2013. Integration of logistic regression, Markov chain and cellular automata models to simulate urban expansion. Int. J. Appl. Earth Obs. Geoinf. 21, 265–275.
Asgarian, A., Amiri, B.J., Sakieh, Y., 2014. Assessing the effect of green cover spatial patterns on urban land surface temperature using landscape metrics approach. Urban Ecosyst. 18 (1), 209–222.
Bozkaya, A.G., Balcik, F.B., Goksel, C., Esbah, H., 2015. Forecasting land cover growth using remotely sensed data: a case study of the Igneada protection area in Turkey. Environ. Monit. Assess. 187, 59.
Brown, D.G., Pijanowski, B.C., Duh, J.D., 2000. Modelling the relationships between land use and land cover on private lands in the Upper Midwest, USA. J. Environ. Manage. 59 (4), 247–263.
Bürgi, M., Hersperger, A., Schneeberger, N., 2004. Driving forces of landscape change - current and new directions. Landsc. Ecol. 19 (8), 857–868.
Camacho Olmedo, M.T., Paegelow, M., Mas, J., Escobar, F., 2018. Geomatic approaches for modeling land change scenarios. In: Cartwright, W., Gartner, G., Meng, L., Peterson, M.P. (Eds.), Lecture Notes in Geoinformation and Cartography. Springer International Publishing AG, Cham, Switzerland.
Cao, Y., Zhang, X., Fue, Y., Lu, Z., Sheng, X., 2020. Urban spatial growth modeling using logistic regression and cellular automata: a case study of Hangzhou. Ecol. Indic. 113, 106200.
Capitani, C., Van Soesbergen, A., Mukama, K., Malugu, I., Mbilinyi, et al., 2019. Scenarios of land use and land cover change and their multiple impacts on natural capital in Tanzania. Environ. Conserv. 46, 17–24.
Chakraborti, S., Das, D.N., Mondal, B., Shafizadeh-Moghadam, H., Feng, Y., 2018. A neural network and landscape metrics to propose a flexible urban growth boundary: a case study. Ecol. Indic. 93, 952–965.
Chapman, S., Watson, J.E.M., Salazar, A. Marcus, Thatcher, M., McAlpine, C.A., 2017. The impact of urbanization and climate change on urban temperatures: a systematic review. Landsc. Ecol. 32 (10), 1921–1935.
Congalton, R.G., Green, K., 1999. Assessing the accuracy of remotely sensed data: principles and practices. CRC/Lewis Press, Boca Raton.
Cushman, S.A., McGarigal, K., Neel, M.C., 2008. Parsimony in landscape metrics: strength, universality, and consistency. Ecol. Indic. 8 (5), 691–703.
Dezhkam, S., Amiri, B.J., Darvishsefat, A.A., Sakieh, Y., 2017. Performance evaluation of land change simulation models using landscape metrics. Geocarto Int. 32 (6), 655–677.
Du, G., Shin, K.J., Yuan, L., Managi, S., 2018. A comparative approach to modelling multiple urban land use changes using tree-based methods and cellular automata: the case of Greater Tokyo area. Int. J. Geogr. Inf. Sci. 32 (4), 757–782.
Eastman, J.R., 2006. IDRISI Andes tutorial. Clark Labs, Worcester.
Eastman, J.R., Van Fossen, M.E., Solorzano, L.A., 2005. Transition Potential Modeling for Land Cover Change. In: Maguire, D., Batty, M., Goodchild, M. (Eds.), GIS, Spatial Analysis and Modeling. Redlands, CA, ESRI Press, pp. 357–386.
Fahrig, L., 2002. Effects of habitat fragmentation on the extinction threshold: a synthesis. Ecol. Appl. 12 (2), 346–353.
Farina, A., 2006. Principles and methods in landscape ecology: toward a science of landscape. Springer Publication, Netherland, p. 412.
Foley, J.A., DeFries, R., Asner, G.P., Barford, C., Bonan, G., Carpenter, S.R., Chapin, F.S., Coe, M.T., Daily, G.C., Gibbs, H.K., Helkowski, J.H., Holloway, T., Howard, E.A., Kucharik, C.J., Monfreda, C., Patz, J.A., Prentice, I.C., Ramankutty, N., Snyder, P.K., 2005. Global consequences of land use. Science 309, 570–574.
Frazier, A.E., Kedron, P., 2017. Landscape metrics: past progress and future directions. Curr. Landsc. Ecol. Rep. 2, 63–72.
Guan, D., Li, H., Inohae, T., Su, W., Nagaie, T., Hokao, K., 2011. Modeling urban land use change by the integration of cellular automaton and Markov model. Ecol. Modell. 222 (20–22), 3761–3772.
Guidigan, M.L.G., Sanou, C.L., Ragatoa, D.S., Fafa, C.O., Mishra, V.N., 2019. Assessing land Use/Land cover dynamic and its impact in Benin Republic using land change model and CCI-LC products. Earth Syst. Environ. 3 (1), 127–137.
Gupta, R., Sharma, L.K., 2020. Efficacy of Spatial Land Change Modeler as a forecasting indicator for anthropogenic change dynamics over five decades: a case study of Shoolpaneshwar Wildlife Sanctuary, Gujarat, India. Ecol. Indic. 112, 106171.
Hamad, R., Balzter, H., Kolo, K., 2018. Predicting land use/land cover changes using a CA-Markov model under two different scenarios. Sustainability 10 (10), 3421.
Islam, K., Rahman, M.F., Jashimuddin, M., 2018. Modeling land use change using Cellular Automata and Artificial Neural Network: the case of Chunati Wildlife Sanctuary, Bangladesh. Ecol. Indic. 88, 439–453.

Jaafari, S., Sakieh, Y., Shabani, A.A., Danehkar, A., Nazarisamani, A., 2015. Landscape change assessment of reservation areas using remote sensing and landscape metrics (case study: Jajroud reservation Iran). Environ. Dev. Sustain. 18 (6), 1701–1717.
Jiang, G.H., Zhang, F.R., Kong, X.B., 2009. Determining conversion direction of the rural residential land consolidation in Beijing mountainous areas. Trans. Chin. Soc. Agric. Eng. 25 (2), 214–221.
Kantakumar, L.N., Kumar, S., Schneider, K., 2019. SUSM: a scenario-based urban growth simulation model using remote sensing data. Eur. J. Remote Sens. 52 (S2), 26–41.
Kolb, M., Mas, J.-F., Galiciac, L., 2013. Evaluating drivers of land-use change and transition potential models in a complex landscape in Southern Mexico. Int. J. Geogr. Inf. Sci. 27 (9), 1804–1827.
Kong, F., Yin, H., Nakagoshi, N., Philip, James P., 2012. Simulating urban growth processes incorporating a potential model with spatial metrics. Ecol. Indic. 20, 82–91.
Kumar, M., Denis, D.M., Singh, S.K., Szilárd Szabó, S., Suryavanshi, S., 2018. Landscape metrics for assessment of land cover change and fragmentation of a heterogeneous watershed. Remote Sens. Appl: Soc. Environ. 10, 224–233.
Lambin, E.F., Geist, H.J., Lepers, E., 2003. Dynamics of land-use and land-cover change in tropical regions. Annu. Rev. Environ. Resour. 28, 205–241.
Le, Q.B., Park, S.J., Vlek, P.L.G., Cremers, A.B., 2008. Land-use dynamic simulator (LUDAS): a multi-agent system model for simulating spatio-temporal dynamics of coupled human-landscape system. I. Structure and theoretical specification. Ecol. Inf. 3 (2), 135–153.
Lechner, A.M., Langford, W.T., Bekessy, S.A., Jones, S.D., 2012. Are landscape ecologists addressing uncertainty in their remote sensing data? Landsc. Ecol. 27, 1249–1261.
Li, Z.T., Li, M., Xia, B.C., 2020. Spatio-temporal dynamics of ecological security pattern of the Pearl River Delta urban agglomeration based on LUCC simulation. Ecol. Indic. 114, 106319.
Liu, B., Chen, S., Liu, H., Guan, Y., 2020. Changes in the ratio of benthic to planktonic diatoms to eutrophication status of Muskegon Lake through time: implications for a valuable indicator on water quality. Ecol. Indic. 114, 106284.
Liu, Y., Li, L., Chen, L., Cheng, L., Zhou, X., Cui, Y., Li, H., Liu, W., 2019. Urban growth simulation in different scenarios using the SLEUTH model: a case study of Hefei, East China. PLoS One 14 (11), e0224998.
McGarigal, K., Cushman, S. A., Ene, E., 2012. FRAGSTATS v4: Spatial Pattern Analysis Program for Categorical and Continuous Maps. Computer software program produced by the authors at the University of Massachusetts, Amherst. Available at http://www.umass.edu/landeco/research/fragstats/fragstats.html.
McGarigal, K., Cushman, S.A., Neel, M.C., Ene, E., 2002. FRAGSTATS: spatial pattern analysis program for categorical maps. Amherst: Computer software program produced by the authors at the University of Massachusetts. Available from http://www.umass.edu/landeco/research/fragstats/fragstats.html.
Mirkatouli, J., Hosseini, A., Neshat, A., 2015. Analysis of land use and land cover spatial pattern based on Markov chains modelling. City, Territ. Archit. 2, 4.
Mishra, V.N., Rai, P.K., 2016. A remote sensing aided multi-layer perceptron-Markov chain analysis for land use and land cover change prediction in Patna district (Bihar), India. Arab. J. Geosci. 9 (4), 1–18.
Mishra, V.N., Rai, P.K., Prasad, R., Punia, M., Nistor, M.M., 2018. Prediction of spatio-temporal land use/land cover dynamics in rapidly developing Varanasi district of Uttar Pradesh, India using Geospatial approach: a comparison of hybrid models. Appl. Geomat. 10 (3), 257–276.
Mishra, V.N., Rai, P.K., Mohan, K., 2014. Prediction of land use changes based on land change modeler (LCM) using remote sensing: a case study of Muzaffarpur (Bihar), India. J. Geogr. Inst. Jovan Cvijic. 64 (1), 111–127.
Mitsova, D., Shuster, W., Wang, X., 2011. A cellular automata model of land cover change to integrate urban growth with open space conservation. Landsc. Urban Plan. 99 (2), 141–153.
Mmbaga, N.E., Munishi, L.K., Treydte, A.C., 2017. How dynamics and drivers of land use/ land cover change impact elephant conservation and agricultural livelihood development in Rombo, Tanzania. J. Land Use Sci. 12 (2–3), 168–181.
Nasiri, V., Darvishsefat, A.A., Rafiee, R., Shirvany, A., Hemat, M.A., 2019. Land use change modeling through an integrated Multi-Layer Perceptron Neural Network and Markov Chain analysis (case study: Arasbaran region, Iran). J. For. Res. 30 (3), 943–957.
Omar, P.J., Dwivedi, S.B., Dikshit, P.K.S., 2020. Sustainable Development and Management of Groundwater in Varanasi, India. In: Alkhaddar, R., Singh, R.K., Dutta, S., Kumari, M. (Eds.), Advances in Water Resources Engineering and Management. Lecture Notes in Civil Engineering. Springer, Singapore, pp. 201–209.
Ostad-Ali-Askar, K., Su, R., Liu, L., 2018. Water resources and climate change. J. Water Clim. Change 9 (2), 239.
Ostad-Ali-Askari, K., Kharazi, H.G., Shayannejad, M., Zareian, M.J., 2019. Effect of management strategies on reducing negative impacts of climate change on water resources of the Isfahan-Borkhar aquifer using MODFLOW. River Res. Appl. 35 (6), 611–631.
Ostad-Ali-Askari, K., Kharazi, H.G., Shayannejad, M., Zareian, M.J., 2020. Effect of climate change on precipitation patterns in an arid region using GCM models: case study of Isfahan-Borkhar Plain. Nat. Hazards Rev. 21, 04020006. https://doi.org/10.1061/(ASCE)NH.1527-6996.0000367.
Ostad-Ali-Askari, K., Shayannejad, M., Eslamian, S., Zamani, F., Shojaei, N., Navabpour, B., Majidifar, Z., Sadri, A., Ghasemi-Siani, Z., Nourozi, H., Vafaei, O., Homayouni, S. M.A., 2017. Deficit irrigation: optimization models. In. Handbook of Drought and Water Scarcity, Management of Drought and Water Scarcity, Saeid Eslamian, Faezeh Eslamian (Eds.), 3, 373-389, Taylor & Francis Publisher. Imprint: CRC Press, Boca Raton.
Pandey, M.K., 2014. Confluence Dynamics of Lower Son River with River Ganga: Tectonic and Climatic Perspective; Unbpublished. Ph.D. Thesis. Banaras Hindu University, Varanasi.
Paudel, S., Yuan, F., 2012. Assessing landscape changes and dynamics using patch analysis and GIS modeling. Int. J. Appl. Earth Obs. Geoinf. 16, 66–76.
Peng, J., Wang, Y.L., Zhang, Y., Wu, J.S., Li, W.F., You Li, Y., 2010. Evaluating the effectiveness of landscape metrics in quantifying spatial patterns. Ecol. Indic. 10 (2), 217–223.
Pirnazar, M., Hasheminasab, H., Karimi, A.Z., Ostad-Ali-Askari, K., Ghasemi, Z., Hamedani, M.H., Esfahani, E.M., Eslamian, S., 2018. The evaluation of the usage of the fuzzy algorithms in increasing the accuracy of the extracted land use maps. Int. J. Glob. Environ. 17 (4), 307–321.
Pontius Jr., R.G., Millones, M., 2011. Death to Kappa: birth of quantity disagreement and allocation disagreement for accuracy assessment. Int. J. Remote Sens. 32 (15), 4407–4429.
Pontius Jr., R.G., Batchu, K., 2003. Using the relative operating characteristic to quantify certainty in prediction of location of land cover change in India. Trans. GIS 7 (4), 467–484.
Pontius Jr., R.G., Si, K., 2014. The total operating characteristic to measure diagnostic ability for multiple thresholds. Int. J. Geogr. Inf. Sci. 28 (3), 570–583.
Prajapati, S.K., Tripathi, B.D., 2008. Assessing the genotoxicity of urban air pollutants in Varanasi City using Tradescantia micronucleus (Trad-MCN) bioassay. Environ. Int. 34, 1092–1096.
Prasad, P.R.C., Rajan, K.S., Dutt, C.B.S., Roy, P.S., 2010. A conceptual framework to analyse the land-use/land-cover changes and its impact on phytodiversity: a case study of North Andaman Islands. India. Biodivers. Conserv. 19, 3073–3087.
Rafiee, R., Mahiny, A.S., Khorasani, N., Darvishsefat, A.A., Danekar, A., 2009. Simulating urban growth in Mashad city, Iran through the SLEUTH model (UGM). Cities 26 (1), 19–26.
Raju, K.N.P., Bhatt, D., 2015. Water in ancient Indian perspective and ponds of Varanasi as water harvesting structures. In: Raju, N.J., Gossel, W., Ramanathan, A.L., Sudhakar, M. (Eds.), Management of Water, Energy and Bio-Resources in the Era of Climate Change: Emerging Issues and Challenges. Springer Cham, pp. 63–71.
Raju, K.N.P., Pandey, M.K., 2013, Varanasi: Origin and Growth from a Geomorphic Perspective, In Varanasi: Myths and Scientific Studies, pp. 134–150. Ed Vidula Jayaswal. Delhi: Aryan Books International, New Delhi; 8173054509/9788173054501.
Raju, K.N.P., Sarkar, S., Pandey, M.K., 2015. Indus and Ganga River Basins in India: Surface Water Potentials, In Water Resources: Rejuvenation of Surface Water Resources of India: Potential, Problems and Prospects, pp. 43–53. Ed R. Vaidyanadhan. Geological Society of India, Bangalore, India; 978-93-80998-04-6.
Reynolds, M., 2014. Life Along the Ganga: Varanasi.
Sakieh, Y., Salmanmahiny, A., 2016. Performance assessment of geospatial simulation models of land-use change-a landscape metric-based approach. Environ. Monit. Assess. 188, 169.
Sakieh, Y., Salmanmahiny, A., Jafarnezhad, J., Mehri, A., Kamyab, H., Galdavi, S., 2015. Evaluating the strategy of decentralized urban land-use planning in a developing region. Land Use Policy 48, 534–551.
Salehi-Hafshejani, S., Shayannejad, M., Broujeni, H.S., Zarraty, A.R., Soltani, B., Esfahani, E.M., Hamedani, M.H., Eslamian, S., Askari, K.O.A., 2019. Determination of the height of the vertical filter for heterogeneous Earth dams with vertical clay core. Int. J. Hydrol. Sci. Technol. 9 (3), 221–235.
Sallustio, L., De Toni, A., Strollo, A., Di Febbraro, M., Gissi, E., Casella, L., Geneletti, D., Munafò, M., Vizzarri, M., Marchetti, M., 2017. Assessing habitat quality in relation to the spatial distribution of protected areas in Italy. J. Environ. Manage. 201, 129–137.
Shukla, U.K., 2013. Varanasi and the Ganga river: a geological perspective. Varanasi, Myth. Sci. Stud. 100–113.
Singh, A., 2015. Observations on the Flora of Varanasi District in Uttar Pradesh State of India. Glob. J. Environ. Sci. Technol. 3, 368–389.
Singh, R.L., Singh, K.N., 1971. Middle Ganga Plain. In: India: A Regional Geography. National Geographical Society of India, Varanasi, India, pp. 247–248.
Smiraglia, D., Ceccarelli, T., Bajocco, S., Perini, L., Salvati, L., 2015. Unraveling landscape complexity: land use/land cover changes and landscape pattern dynamics (1954–2008) in contrasting peri-urban and agro-forest regions of northern Italy. Environ. Manage. 56, 916–932.
Szilassi, P., Jordan, G., Van Rompaey, A., Csillag, G., 2006. Impacts of historical land use changes on erosion and agricultural soil properties in the Kali Basin at Lake Balaton, Hungary. Catena 68 (2–3), 96–108.
Tan, F.-S., Song, H.-Q., Fu, P.-L., Chen, Y.-J., Siddiq, Z., Cao, K.-F., Zhu, S.-D., 2020. Hydraulic safety margins of co-occurring woody plants in a tropical karst forest experiencing frequent extreme droughts. Agric. For. Meteorol. 292–293, 108107.
Tang, J., Di, L., 2019. Past and future trajectories of farmland loss due to rapid urbanization using Landsat imagery and the Markov-CA model: a case Study of Delhi. India. Remote Sens. 11 (2), 180.
Triantakonstantis, D., Mountrakis, G., 2012. Urban growth prediction: a review of computational models and human perceptions. J. Geogr. Inf. Syst. 4, 555–587.
Trombulak, S.C., Frissell, C.A., 2000. Review of ecological effects of roads on terrestrial and aquatic communities. Conserv. Biol. 14, 18–30.
Tsarouchi, G.M., Mijic, A., Moulds, S., Buytaert, W., 2014. Historical and future land-cover changes in the Upper Ganges basin of India. Int. J. Remote Sens. 35 (9), 3150–3176.
Turner, B.L., 2010. Sustainability and forest transitions in the southern Yucatán: the land architecture approach. Land Use Policy 27 (2), 170–179.

Varga, O.G., Pontius Jr., R.G., Singh, S.K., Szaboa, S., 2019. Intensity analysis and the Figure of Merit's components for assessment of a Cellular Automata–Markov simulation model. Ecol. Indic. 101, 933–942.
Verburg, P.H., Paul, P.S., Martin, J. Dijst, Veldkamp, A., 2004. Land use change modelling: current practice and research priorities. GeoJournal 61 (4), 309–324.
Wu, J., Hobbs, R., 2002. Key issues and research priorities in landscape ecology: an idiosyncratic synthesis. Landsc. Ecol. 17, 355–365.
Wu, X., Hu, Y., He, H.S., Bu, R., Onsted, J., Xi, F., 2009. Performance evaluation of the SLEUTH model in the Shenyang metropolitan area of Northeastern China. Environ. Monit. Assess. 14, 221–230.
Yao, Y., Liu, X., Li, X., Liu, P., Hong, Y., Zhang, Y., Mai, K., 2017. Simulating urban land-use changes at a large scale by integrating dynamic land parcel subdivision and vector-based cellular automata. Int. J. Geogr. Inf. Sci. 31 (12), 2452–2479.